HOKKAIDO UNIVERSITY

Title	Study on Force-Induced Polymerization and Growth in Double-Network Hydrogels with Vascular-Like Monomer Supply
Author(s)	魏, 谷米
Degree Grantor	北海道大学
Degree Name	博士(ソフトマター科学)
Dissertation Number	甲第16037号
Issue Date	2024-06-28
DOI	https://doi.org/10.14943/doctoral.k16037
Doc URL	https://hdl.handle.net/2115/92915
Type	doctoral thesis
File Information	Gumi_WEI.pdf

Hokkaido University Collection of Scholarly and Academic Papers : HUSCAP

Doctoral Dissertation

Study on Force-Induced Polymerization and Growth in Double-Network Hydrogels with Vascular-Like Monomer Supply

（血管様モノマー供給を有するダブルネットワークゲルにおける力誘発重合と成長に関する研究）

Gumi WEI

Laboratory of Soft and Wet Matter

Division of Soft Matter

Graduate School of Life Science, Hokkaido University, Japan

June 2024

Content

Content i

List of Important Abbreviations iv

Chapter 1 General Introduction 1

1.1. Overview 1

1.1.1. Introduction 1

1.1.2. Current Issues 2

1.1.3. Purpose and Significance 3

1.2. Outline 4

1.3. References 6

Chapter 2 Background 9

2.1. Fracture in Mechanochemical Subjects 9

2.2. Double-Network (DN) Hydrogels as Mechanochemical Subjects 10

2.2.1. Double-Network Hydrogel 10

2.2.2. Force-Induced Mechanoradicals in DN Gel 11

2.2.3. Self-Growth of DN Gel 13

2.3. Vascular Structures in Synthetic Materials 15

2.4. Summary and Prospects 16

2.5. References 20

Chapter 3 Channel Structures in DN Gel 30

3.1. Introduction 30

3.2. Experiments 31

3.2.1. Materials 31
3.2.2. 3D Printed Capillary Tube Mold.....31
3.2.3. Synthesis of PNaAMPS Gel with Channel.....31
3.2.4. Synthesis of Channel-Integrated Double-Network (c-DN) Hydrogel 32
3.2.5. Diffusion Measurement Using ATR FT-IR.....32
3.3. Results and Discussion 33
3.3.1. c-DN Gel and Circulatory System 33
3.3.2. Diffusion Through the Vascular-Like Channel.....33
3.4. Conclusions.....34
3.5. Reference 41
Chapter 4 Mechanoradical Polymerization in c-DN Gel 43
4.1. Introduction.....43
4.2. Experiments 43
4.2.1. Materials 43
4.2.2. Evaluation of Mechanoradical Concentration by Fenton Color Reaction .43
4.2.3. Preparation of fluorescence spectroscopy sample 44
4.2.4. Fluorescence observation using LSCM 45
4.3. Results and Discussion 45
4.3.1. Mechanoradical Concentration of c-DN gels 45
4.3.2. Diffusion-Limited Mechanoradical Polymerization 45
4.3.3. Life-time of Mechanoradicals.....47
4.4. Conclusions.....48
4.5. References.....54

Chapter 5 Vascular-Like Channel Sustained Self-Growth 57

5.1. Introduction.....57

5.2. Experiments 58

5.2.1. Self-Growth of c-DN Gel Supplied by Channel Flow.....58

5.2.2. SEM Observation Before and After Self-Growth.....58

5.2.3. Raman Spectroscopy for Detecting Constitution Change 59

5.3. Results and Discussion 59

5.3.1. Muscle-Like Cyclic Strengthening Sustained by Continuous Flow.....59

5.3.2. Tunable Self-Growth in Response to Channel Flow.....61

5.3.3. Volume Growth.....61

5.3.4. Quantification of Mechanical Self-Growth 62

5.3.5. Quantification of Mechanochemical Growth.....63

5.3.6. Delayed Strengthening after Polymer Growth.....64

5.4. Conclusions.....66

5.5. References.....87

Chapter 6 General Conclusion and Outlook.....90

List of Publications 92

Acknowledgement.....93

List of Important Abbreviations

DN	Double-network
c-DN	channel-integrated double-network hydrogel
ATR-FTIR	Attenuated total reflection Fourier transform infrared
MBAA	N,N'-Methylenebisacrylamide
(P)AAm	(Poly) acrylamide
(P)NaAMPS	(Poly) 2-acrylamido-2-methylpropane sulfonic acid sodium salt
(P)NIPAAm	(Poly) N-isopropylacrylamide
UV	Ultraviolet
XO	Xylenol orange
ANS	8-anilino-1-naphthalene sulfonic acid
LCST	Lowest critical solution temperature
LSCM	Laser scanning confocal microscopy
Dp	Displacement

Chapter 1 General Introduction

1.1. Overview

1.1.1. Introduction

Double-network (DN) hydrogels represent a remarkable class of materials with a distinctive polymer network structure.[1] This unique network configuration imparts DN hydrogels with extraordinary mechanical properties and functionality.[2, 3] DN gels are also unique mechanochemical materials in which their structures are able to be dynamically remodeled during use. The mechanical energy applied to DN gels is efficiently transferred to chemical bonds of the brittle network,[4] generating mechanoradicals that initiate the polymerization of pre-loaded monomers, thereby remodeling the materials.[5] Recently, a seminal study contributing to a further understanding of DN hydrogels is conducted, the authors delved into the mechanical intricacies of DN hydrogels, unveiling the fascinating capability of these materials to generate mechanoradicals under stretch, and proposed a strategy for developing "self-growing" polymeric materials that respond to repetitive mechanical stress, and enhance the mechanical performance of DN gel. The mechanical is based upon an effective mechanochemical transduction in DN gels, such enhancement comes from the polymerization of a new network initiated by mechanoradicals, these chain-end radicals generated from the brittle first network chain fracture upon mechanical actions are capable of initiating the mechanoradical polymerization in the hydrogel matrix, while the ductile second network that is highly stretchable insures its integrity and softness.[6]

The revelation of mechanoradical generation potential of DN hydrogels has opened avenues for exploring applications that harness the material, and impart DN

hydrogels or elastomers with a self-growth behavior that mimics muscle training, as a result, the DN gel exhibits a metabolic-like behavior with repeated transductions between chemical energy and mechanical work. Besides, the mechanoradicals generated are able to impart DN hydrogels or elastomers with prolific functional improvements, such as the force stamp-induced surface patterning for cell culture,[7] or mapping the internal fractures by fluorescent mechanophores.[8, 9]

1.1.2. Current Issues

Although the above-mentioned studies have promoted branching of double network concepts into investigations of mechanochemistry, which starts a strategic junction of these two areas, there are still two main problems that baffle further progress of DN gels in the field of mechanochemistry: (1) the requirement of anaerobic condition, and (2) a constant supply to complement the monomer consumption during the force-triggered mechanoradical polymerization is necessary.

To address the previous issue, Wang et al. incorporate an azoalkane crosslinker into the first network of DN gels, the azoalkane crosslinker causes a decrease in the yield stress but significantly increases the mechanoradical concentration of DN gels after stretching, the concentration of mechanoradicals can reach up to 5 times that of the traditional crosslinker. Azoalkane crosslinker introduced weak bonds,[10-12] such strategy in the first network will effectively increase the amount of radicals produced in DN gels after stretching, which is able to accelerate the mechanoradical reactions and lower the allowable limit of oxygen concentration. The second issue mentioned above is primarily involved with the requirement for under-solution environments, that an opening system filled with monomer solution is used to complement monomer consumption during mechanoradical polymerizations. Because the under-solution

system is necessary to support the mechanochemical reactions in DN gel, such experimental conditions result in a circumstance that both the DN gel and the stretching jigs have to be limited in a tub filled with solution of monomers and cross-linkers, which largely confines their observations and usages.

1.1.3. Purpose and Significance

In order to address the above mentioned issue comes from the under-solution complementary system, we intend to construct a self-sustainable system with an independent monomer complementation, freeing the gel from the limitations from the under-solution system.

When we put our eyes on some living organisms, it is easy to find that most biological activities rely on vascular structures.[13] In human body, the circulatory system can transform the nutrients and oxygen into any part of our body and take the wastes out.[14-16] In plants, the water, fertilizer and elements are also delivered from the roots to the leaves by the vascular tissues such as the xylem and phloem, which play an important role in supplying the building blocks for reconstructions.[17-19] These representative vascular structures provide us inspirations for hydrogel–channel integration and explore more possibilities about structural DN gel to be used in various field such as biological mimicry, soft robotic, or mechanical modifiable intelligence material.

Taking inspirations from the vascular system in nature, our purpose is utilizing sacrificial templates to create inner vascular structures embedded in double network hydrogels. The channel in DN gel functions as a delivering pathway inside DN hydrogels, like blood vessels in the human body or vascular tissues in the plant, by which solvents or solutions can be perfused through vascular-like flow through the gel.

By the internal circulatory flow suppling from the channel, it is achievable for the channel-integrated DN (c-DN) hydrogel to sustain itself during the mechanoradical polymerizations. By liquid perfusing inside the channel, the hydrogel is getting free from limitations of the open-system, which need to soak the self-growth system including the whole sample and the loading jig into large amount of solution. The chemicals diffused from the inner flow into the DN gel provide an emulate environment of in-vivo nutrients circulation, which is also a suitable method for tissue mimicking.

1.2. Outline

This dissertation delves into multifaceted aspects of DN hydrogels, exploring their synthesis, characterization, and the underlying mechanisms governing their mechanical and functional behavior. The subsequent chapters will provide a comprehensive overview of the current state of knowledge in this exciting and evolving field.

This dissertation comprises six chapters including this general introduction as **Chapter 1.** In this chapter, a comprehensive analysis of prevailing challenges is presented, we emphasize the essentialities and reasons of the c-DN gel as the structural basis of this dissertation.

In **Chapter2,** the review of current literatures is summarized as a background for our dissertation. We comprehensively review the ongoing explorations, and highlight the distinctive properties of DN hydrogels, note the main strategy behind is the fracture of the brittle network in DN gels. Such bond scission gives capability to generate mechanoradicals under a force trigger, which is especially unique among all the soft matters.

In **Chapter 3**, we introduce the method of constructing a channel inside DN hydrogel. The solution flowing inside the c-DN hydrogel is achieved by the channel

structure, and the chemical signals of monomer molecules diffusion are measured, hence ascertained the time required for a thoroughly penetration of the monomer solution into the hydrogel.

In **Chapter 4**, The c-DN hydrogel is used as a matrix for diffusion limited in-situ mechanoradical polymerization, the internal channel functions as a delivering pathway to provide the monomers. Besides, the diffusion process visualized by fluorescent will provide a time scale for diffusion from the channel wall to the outer surface of c-DN gels. After referring to the time scale of diffusion, we can deduce the life-time of mechanoradicals.

In **Chapter 5**, further attempts is made by using the channel structure to supply monomers for mechanoradical polymerization. Notably, when subjected to cyclic tensile forces, c-DN hydrogels exhibit a tunable self-strengthening according to the concentration and time of vascular perfusion. Both the amount and kinetics of the mechanical and chemical growth is studied, and a delayed strengthening after self-growth is discovered.

In **Chapter 6**, conclusions of this research are summarized

1.3. References

1 J. P. Gong, “Why are double network hydrogels so tough?”, *Soft Matter*, 2010, **6**, 2583-2590.

2 R. J. Song, X. Y. Wang, M. Johnson, C. Milne, A. Lesniak-Podsiadlo, Y. H. Li, J. Lyu, Z. S. Li, C. Y. Zhao, L. Z. Yang, I. Lara-Sáez, A. Sigen and W. X. Wang, “Enhanced Strength for Double Network Hydrogel Adhesive Through Cohesion-Adhesion Balance”, *Advanced Functional Materials*, 2024, DOI: 10.1002/adfm.202313322.

3 Y. H. Na, T. Kurokawa, Y. Katsuyama, H. Tsukeshiba, J. P. Gong, Y. Osada, S. Okabe, T. Karino and M. Shibayama, “Structural characteristics of double network gels with extremely high mechanical strength”, *Macromolecules*, 2004, **37**, 5370-5374.

4 K. Fukao, T. Nakajima, T. Nonoyama, T. Kurokawa, T. Kawai and J. P. Gong, “Effect of Relative Strength of Two Networks on the Internal Fracture Process of Double Network Hydrogels As Revealed by Small-Angle X-ray Scattering”, *Macromolecules*, 2020, **53**, 1154-1163.

5 T. Matsuda, R. Kawakami, R. Namba, T. Nakajima and J. P. Gong, “Mechanoresponsive self-growing hydrogels inspired by muscle training”, *Science*, 2019, **363**, 504-508.

6 T. Nakajima, H. Furukawa, Y. Tanaka, T. Kurokawa, Y. Osada and J. P. Gong, “True Chemical Structure of Double Network Hydrogels”, *Macromolecules*, 2009, **42**, 2184-2189.

7 Q. F. Mu, K. P. Cui, Z. J. Wang, T. Matsuda, W. Cui, H. Kato, S. Namiki, T. Yamazaki, M. Frauenlob, T. Nonoyama, M. Tsuda, S. Tanaka, T. Nakajima and J. P. Gong, “Force-triggered rapid microstructure growth on hydrogel surface for on-demand functions”, *Nature Communications*, 2022, **13**, 6213.

8 E. Ducrot, Y. L. Chen, M. Bulters, R. P. Sijbesma and C. Creton, “Toughening Elastomers with Sacrificial Bonds and Watching Them Break”, *Science*, 2014, **344**, 186-189.

9 T. Matsuda, R. Kawakami, T. Nakajima and J. P. Gong, “Crack Tip Field of a Double-Network Gel: Visualization of Covalent Bond Scission through Mechanoradical Polymerization”, *Macromolecules*, 2020, **53**, 8787-8795.

10 G. Kim, Q. Wu, J. L. Chu, E. J. Smith, M. L. Oelze, J. S. Moore and K. C. Li, “Ultrasound controlled mechanophore activation in hydrogels for cancer therapy”, *Proceedings of the National Academy of Sciences of the United States of America*, 2022, **119**, 2109791119.

11 B. Lee, Z. B. Niu, J. P. Wang, C. Slebodnick and S. L. Craig, “Relative Mechanical Strengths of Weak Bonds in Sonochemical Polymer Mechanochemistry”, *Journal of the American Chemical Society*, 2015, **137**, 10826-10832.

12 K. L. Berkowski, S. L. Potisek, C. R. Hickenboth and J. S. Moore, “Ultrasound-induced site-specific cleavage of azo-functionalized poly(ethylene glycol)”, *Macromolecules*, 2005, **38**, 8975-8978.

13 M. K. Pugsley and R. Tabrizchi, “The vascular system - An overview of structure and function”, *Journal of Pharmacological and Toxicological Methods*, 2000, **44**, 333-340.

14 V. S. H. Rao and T. S. L. Radhika, “The Dynamics of the Flow of Blood in the Human Circulatory System”, *Differential Equations and Dynamical Systems*, 2023, **31**, 673-685.

15 Y. M. Cheng, X. L. Liu, X. T. Ma, R. Garcia, K. Belfield and J. Haorah, “Alcohol promotes waste clearance in the CNS via brain vascular reactivity”, *Free Radical Biology and Medicine*, 2019, **143**, 115-126.

16 H. M. Wei, H. M. Jiang, Y. F. Zhou, X. C. Xiao, C. Zhou and X. M. Ji, “Vascular endothelial cells: a fundamental approach for brain waste clearance”, *Brain*, 2023, **146**, 1299-1315.

17 J. H. Jung and C. M. Park, “Vascular development in plants: Specification of xylem and phloem tissues”, *Journal of Plant Biology*, 2007, **50**, 301-305.

18 R. R. McKenzie and M. K. Deyholos, “Effects of plant growth regulator treatments on stem vascular tissue development in linseed”, *Industrial Crops*

and Products, 2011, **34**, 1119-1127.

19 B. De Rybel, M. Adibi, A. S. Breda, J. R. Wendrich, M. E. Smit, O. Novák, N. Yamaguchi, S. Yoshida, G. Van Isterdael, J. Palovaara, B. Nijsse, M. V. Boekschoten, G. Hooiveld, T. Beeckman, D. Wagner, K. Ljung, C. Fleck and D. Weijers, "Plant developement Integration of growth and patterning during vascular tissue formation in Arabidopsis", *Science*, 2014, **345**, 1255215.

Chapter 2 Background

2.1. Fracture in Mechanochemical Subjects

In most commonly used conventional polymeric materials, the occurrence of fractures in materials is a significant concern that frequently lead to detrimental outcomes.[1-3] In materials like rubbers, the formation of small crazes, although seemingly inconspicuous, may eventually grow to larger structural defects, increasing the potential to evolve into extensive failures, and compromising the overall integrity and performance of the material.[4-8] For a whole set of equipment in practical usages, outages may happen provided that a single rubber part fractures, cracks formation and growth in plastics will also make our products fall into disuse. An inevitable fact is that, for those materials that are frequently subject to mechanical distortions, the mechanical performance decreases as cracks grow and accumulate, their use is therefore limited. To solve these frustrating dissipations, attempts have never ended to develop materials with enhanced durability and resilience,[9-14] and understand the mechanisms behind such fracture processes.[15-22]

The genesis of the groundbreaking realm of fracture-induced chemistry in polymers, as posited in the seminal proposition by Melville and Murray,[23] is that the rupture of a polymer chain could engender radical species—termed mechanoradicals, at the termini of the fractured polymer. The specific definition of mechanochemistry was formulated by Heinicke in 1984, which was described as a branch of chemistry that influences or induces the chemical and physical transformation of substances by mechanical actions.[24] Until now, mechanochemical strategies have been widely studied in polymer science, bringing about results of mechano-responsive functionalities

ranging from damage zone mapping[25] to mechanical strengthening[26] or mechanochemical reactions[27, 28]. For example, H. Tarik Baytekin et al.[29] found that macroscopically reversible deformation of polymers in contact with water produces hydrogen peroxide, and indicated that all the reactions observed from hydrogen peroxide generation such as reduction of gold(III) salt, oxidative bleaching of an aqueous solution of neutral red dye, or fluorescent umbelliferone produced in solution by cleavage of a boronic ester derivative do not occur in the unsqueezed polymers. Which are congruent with the proposed mechanism in which radicals that are generated within the polymer react with water or oxygen to ultimately create hydroxyl and/or hydroperoxyl radicals in solution. Actually, not only utilizing mechanoradicals to induce reactions in force-triggered polymer matrix, mechanochemical treatment has also been used to degrade biopolymers and result in desired molecular weights,[30, 31] or adjust the rheological properties of polymers.[32, 33] Mechanochemical reactions in polymers is receiving an increasing attention in the polymer realm.

2.2. Double-Network (DN) Hydrogels as Mechanochemical Subjects

2.2.1. Double-Network Hydrogel

The Double-network (DN) hydrogel stand out as remarkable materials in the realm of polymer science due to its extraordinary polymer network structure. As firstly introduced by J. P. Gong et al. in 2010, the most commonly used DN hydrogel is consist with a brittle, highly-crosslinked polyelectrolyte as the first network, and the second network soft and ductile.[34] The collaboration of two networks with contrasting mechanical properties enables the DN gel as tough as rubbers even with high water content.

As have formulated by authors in the realm of polymer, the exceptional

mechanical properties and extraordinary fracture energy displayed by DN gels are rooted in their unique internal fracture behavior during deformations, where the brittle network undergoes extensive fragmentation into small clusters, exhibiting substantial fracture energy by bond scissions.[16, 35-37] The broken clusters, in turn, serve as multifunctional cross-linkers for the ductile chains, resulting in the strong orientation of the polymer chains in the second polymer network. These features impart exceptional mechanical strength and toughness to the material.

Due to its distinctive mechanical behaviors, DN hydrogel has become a subject of extensive research within the polymer physics community. The distinctiveness of its polymer network structure sets it apart from conventional hydrogels, offering unique mechanical[38] and functional properties.[39-42] Notably, DN hydrogels exhibit large hysteresis in cyclic tensile tests, and during first loading process, specific DN gels show unique yielding behaviors.[43-45] Not only large energy dissipation but also mechanoradical generation is observed due to their internal fracturing caused by the brittle polymer network.

2.2.2. Force-Induced Mechanoradicals in DN Gel

As mentioned in the previous sub-section, a DN hydrogel is made from two interpenetrated networks with contrasting properties; one is hard and brittle, and the other is soft and stretchable.[37, 46] Owing to these contrasting properties, the DN hydrogel are extremely tough, and the chemical bonds of the brittle network are highly susceptible to mechanical stimuli.

As has already proved by pioneering works, the mechanical energy applied to a DN material causes chemical bond scissions in the first network, generating large amounts of mechanoradicals.[25, 29, 47] Because covalent bonds in the DN gel can serve as

intrinsic activation targets in response to a force trigger, it is unnecessary to design complicated mechanophores within polymer chains, the DN gel itself is a simple but efficient mechano-responsive material.[48]

Due to such unique internal fracture characteristic, DN gel is drawing an increasing attention as promising mechanochemical subjects and facilitated numerous intriguing research endeavors. For example, utilizing the Fenton color reaction, Matsuda et al. observed a color change characteristic of the presence of Fe^{3+} in the necked region.[26] Assuming that all types of mechanoradicals generated by bond scission have the same reactivity in the Fenton solution, the mechanoradical concentration in the completely necked DN gel was estimated to be on the order of 10^{-5} M, which is calculated from the Fe^{3+} concentration. Surpassing that of the single-network (SN) gels counterparts which is on the order of 10^{-6} M or less, indicates the privilege standing of DN gels of generating mechanoradicals by deformation.

Based on the above mentioned principle that the cleavage of bonds in the brittle first network will generate chain-end radicals, researchers are able to initiated the pre-loaded monomers in the DN gel, and polymerize new polymers by applying external forces to the gel (**Figure 2.1**). The mechanoradical polymerization hence impart functional improvements such as self-strengthening,[26, 47, 49] force stamp-induced surface patterning,[50] and damage zone mapping in DN gels [25]. Still, there is a significant potential for further increasing the amount of mechanoradicals generated in DN gel. Because a higher concentration of mechanoradicals would further accelerate the reaction rate in DN gel, and mitigate in the requirements for an anaerobic environment for mechanoradical-initiated polymerization. Wang et al. demonstrated an improved mechanoradical concentration attained in azo-crosslinked DN hydrogels, making a step further to broaden the application fields of DN hydrogels as mechanoradicals

generator.[47]

The above-mentioned studies have promoted the branching of double network concepts into investigations of mechanochemistry, which starts a strategic junction of these two areas.

2.2.3. Self-Growth of DN Gel

For those synthetic materials frequently subjected to repeated deformations, bond-breaking is commonly considered to be the reason for mechanical performance decreases, as cracks grow and accumulate, the products will eventually fall into disuse.[51] But biological tissues like the muscles and bones shows totally different results, internal ruptures are sometimes functioning as the trigger of growth and the chance of renewal.[52] For example, the load-bearing on bones leads to cell differentiation[53, 54]; fibril cracks in muscles release signals of structural destruction-reconstruction process.[52, 55, 56] Initiated by the excellent properties of living tissues, researchers are paying more attention to biomimetic materials, of which muscle mimicries are especially fascinating and have flourished in recent years.[57-59]

Although physical properties of synthetic materials can be manipulated by varying compositions and structures, rendering them to be either stretchable or stiff, soft or tough,[60-63] or even mechanically as strong as muscle tissues,[64, 65] a large gap still exists between the performance of muscles and typical synthetic products, as muscles are reactive to force excitations and dynamic in constitutions,[66-68] while typical synthetic materials are passive bulks with consistent components. Only a few examples are available in demonstrating the construction of artificial muscles,[26, 69] impart characteristics that are able to grow and remodel themselves to the material, therefore achieves a transformation of mechanical work into chemical energy during repeated

force triggers.

To impart the material with force sensing ability, mechanochemical tools mentioned above are specifically feasible approaches for materials to recognize and react to mechanical stimuli. As has been proved in pioneering works, mechanochemical reactions in DN gel response perfectly to force stimuli. Such property comes from the unique network structure of DN gel, enables a special fracture behavior under the influence of a tensile force, the rigid first network allows for bond ruptures along with the generation of mechanoradicals, while the second network that is highly stretchable ensures the integrity, therefore enabling the force sensibility at the molecular level before a macroscopic failure happens.[70]

The mechanoradicals generated from the rigid network fracture can initiate polymerizations of monomers pre-loaded in DN gel, the network is therefore fractured first and then remolded again by mechanoradical polymerization of a new polymer network. In the following tensile stretch cycles, the monomers pre-loaded in DN gel or self-grown multi-network hydrogel matrix are functioned as the building blocks for the newly formed polymers. This reconstruction process is similar to the muscle growth, with renewable constructions of muscle fibers and a growing content of the newly formed muscle tissue, where the building blocks are instead of monomer molecules but amino acids or other necessary elements for muscle building.

The mechanoradical generation characteristic makes the DN gel a unique material with metabolic-like growth. When continuously supplied with monomers and crosslinkers, mechanoradical polymerization will construct a new polymer network, as a result, the gel is mechanically enhanced and gradually grows in a similar behavior of training the muscles. It is worth noticing that when the gel is subjected to repeated force-triggers, the newly formed network, can also fractured and generate

mechanoradicals to initiate another cycle of self-growth.

The muscle-like strengthening of DN gel was demonstrated in the work of Dr. Matsuda et al., by the weight lifting ability, although the original weight is too heavy to be lifted, it is gradually reaching to a higher position compared to the previous cycle as the gel is becoming stiffer.[26] However as show in the setup illustrator for DN gel self-growth (**Figure 2.2**), the continuous monomer supply is needed for the repeated self-growths of DN gel, the repeated loading-unloading process is applied in an open system with large amount of monomer solution, which is not suitable for practical uses, and difficult to observe the gel during self-growing.

2.3. Vascular Structures in Synthetic Materials

In the development of building up a material analogous to those materials present in nature, we may get a lot inspirations from biological existences such as elaborate structures, hierarchically arranged tissues, or unceasing regenerations. For example, some plants usually comprise vascular structures arranged along the complex hierarchical architectures. The primary components of vascular tissue in plants are the xylem and phloem, these two tissues transport fluid and nutrients from the roots to the leaves.[71-73] Not only plants are using vascular structures to transport nutrients, for mammals, the circulatory system constructed by blood vessels throughout most part of our entire body plays an important role in nutrients supplements, temperature adjustments, and neurotransmitter deliveries.[74, 75]

But combining biological characters such as internal circulatory system with synthetic material is not an easy task. Because under repeated deformations, internal fractures often cause a reduction in the mechanical performance, and cracks growing in materials will eventually make the product fall into disuse. To address the mechanical

decrease mentioned above, it is worth noting the work of White et al.[76-80] on the fabrication of vascular pathways for damage repair. The authors described structural materials with polymerizable solutions encapsulated in the vascular network. On breakage, the healing agent would released to heal the crack surfaces and recombine the fractured material. Evidently, this repair method relies on significant cracks over vascular structures and efficient leakage of the polymerizable precursor sealed in the vascular structure, which is similar to the healing of skin: bleeding in the wound result in a healing of the tissue.[81]

However, when it comes to the mimicry of muscle tissue, the ability to sense force is of paramount importance, so as to reconstruct the material at the molecular level even before macroscopic failures happens. At this point, the mechanochemistry strategy mentioned in previous sub-sections may provide us feasible approaches to achieve the structural reconstruction in response to mechanical forces. Specifically, such method provides an avenue to recognize force, not at the macroscopic level, but through the mechanochemical reactions from a chemical point of view.[82-84]

2.4. Summary and Prospects

Muscle building is a metabolic-process in which mechanical work is used to trigger chemical reactions for muscle hypertrophy. The metabolic growth in the muscle fibers provides a fascinating model for material innovations, attracting researchers to build up artificial muscles that are able to grow and remodel themselves according to changes in mechanical and chemical environments. The mechanochemical strategy for DN hydrogel growth arises from their intriguing capability to generate mechanoradicals from fracture of the brittle polymer network, impart DN gels with a fascinating self-growing behavior under mechanical stress. However, to sustain mechanoradical

polymerizations in DN gels, it is necessary to immerse the DN hydrogel in monomer solutions to complement the consumed monomers.

Although gel samples cultured in a monomer solution system showcase of cells and tissues cultured in an extracellular matrix,[85-90] which continuously remodel themselves through metabolic processes fueled by environmental nutrients and allows them to reshape and strengthen. The essential reliance on monomer solutions simultaneously limits their observation and practical applications. Therefore it is necessary for explorations to find another way of providing monomers and crosslinkers for a continuous mechanoradical polymerization. To furtherly broaden the usages of DN gel as a muscle mimicking materials, we need to construct a self-sustainable system with an independent monomer complementation, freeing the gel from the limitations from the under-solution system.

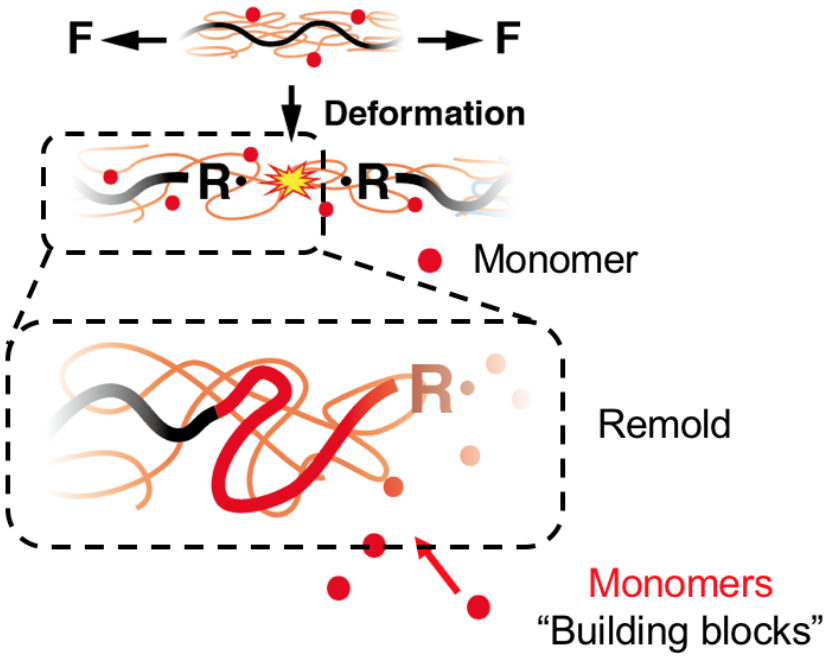


Figure 2.1. Mechanism of the mechanoradical polymerization: stretching of the DN gel triggers internal fracturing of the rigid network, generating chain-end radicals and initiating the polymerization of monomers to form new polymers. Monomers diffused from the open system filled with the monomer solution, therefore replenish monomer consumptions during the mechanoradical polymerization.

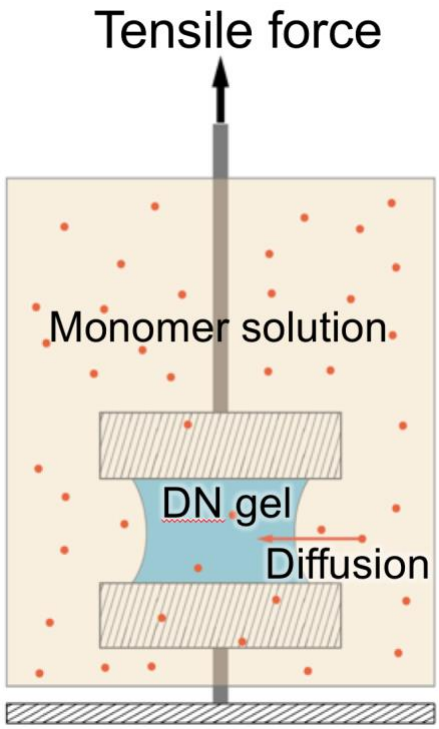


Figure 2.2. Muscle-like strengthening of DN gel applied in an open-system filled with monomer solutions.

2.5. References

1 C. Creton, E. J. Kramer, C. Y. Hui and H. R. Brown, "Failure Mechanisms of Polymer Interfaces Reinforced with Block Copolymers", *Macromolecules*, 1992, **25**, 3075-3088.

2 Y. M. Boiko and R. I. Mamalimov, "On the fracture mechanism of partially healed interfaces of glassy polymers: an ATR-FTIR investigation", *Colloid and Polymer Science*, 2014, **292**, 1003-1007.

3 A. Filip, O. V. Badulescu, P. D. Sirbu, B. Veliceasa, B. Puha, I. A. Pascal, L. Andrusca, S. Oprea, C. Filip and O. Alexa, "Preliminary Investigation on Mechanical Properties of Polymer Coating Screws for the Future Fragility Fracture Fixation", *Materiale Plastice*, 2019, **56**, 559-562.

4 G. H. Michler, M. Ensslen, F. J. Baltá-Calleja, L. Könczöl and W. Döll, "Mechanical properties of crazes investigated by ultramicrohardness", *Philosophical Magazine a-Physics of Condensed Matter Structure Defects and Mechanical Properties*, 1999, **79**, 167-178.

5 C. C. Hsiao and J. A. Sauer, "On Crazing of Linear High Polymers", *Journal of Applied Physics*, 1950, **21**, 1071-1083.

6 A. F. Yee and M. A. Maxwell, "Mechanical-Properties of Polymer Mixtures - Effect of Compatibility", *Journal of Macromolecular Science-Physics*, 1980, **B17**, 543-564.

7 R. J. Morgan, J. E. Oneal and D. L. Fanter, "Effect of Moisture on the Physical and Mechanical Integrity of Epoxies", *Journal of Materials Science*, 1980, **15**, 751-764.

8 G. H. Michler, "Correlation between Craze Formation and Mechanical-Behavior of Amorphous Polymers", *Journal of Materials Science*, 1990, **25**, 2321-2334.

9 T. Chalklen, M. Smith and S. Kar-Narayan, "Improved fatigue resistance in transfer-printed flexible circuits embedded in polymer substrates with low melting temperatures", *Flexible and Printed Electronics*, 2023, **8**, 025014.

10 X. J. Wang and D. D. L. Chung, “Real-time monitoring of fatigue damage and dynamic strain in carbon fiber polymer-matrix composite by electrical resistance measurement”, *Smart Materials and Structures*, 1997, **6**, 504-508.

11 X. J. Wang and D. D. L. Chung, “Fiber breakage in polymer-matrix composite during static and fatigue loading, observed by electrical resistance measurement”, *Journal of Materials Research*, 1999, **14**, 4224-4229.

12 M. Desai, R. Bakhshi, Z. You, A. Seifalian and G. Hamilton, “Thermo-mechanical resistance of a nanocomposite polymer exposed to simulated fatigue in the development of an endovascular stent-graft”, *British Journal of Surgery*, 2011, **98**, 52-53.

13 M. Y. Desai, R. Bakhshi, A. Darbyshire, M. Ahmed, J. Eaton-Evans, X. Zhou, Z. You, A. M. Seifalian and G. Hamilton, “Thermo-Mechanical Resistance of a Nanocomposite Polymer Exposed to Simulated in Vivo Hydrodynamic Fatigue for Ten Years in Developement of a Sutureless Endovascular Stent Graft”, *Journal of Vascular Surgery*, 2011, **53**, 86s-87s.

14 T. Takeda, Y. Shindo, Z. J. Wei, Y. Kuronuma and F. Narita, “Fatigue failure and electrical resistance behaviors of carbon nanotube-based polymer composites under uniaxial tension-tension loading in a cryogenic environment”, *Journal of Composite Materials*, 2015, **49**, 457-463.

15 R. R. McKenzie and M. K. Deyholos, “Effects of plant growth regulator treatments on stem vascular tissue development in linseed”, *Industrial Crops and Products*, 2011, **34**, 1119-1127.

16 K. Fukao, T. Nakajima, T. Nonoyama, T. Kurokawa, T. Kawai and J. P. Gong, “Effect of Relative Strength of Two Networks on the Internal Fracture Process of Double Network Hydrogels As Revealed by Small-Angle X-ray Scattering”, *Macromolecules*, 2020, **53**, 1154-1163.

17 G. V. Vinogradov, “Viscoelasticity and Fracture Phenomenon in Uniaxial Extension of High-Molecular Linear Polymers”, *Rheologica Acta*, 1975, **14**, 942-954.

18 K. L. Devries, “Review of Techniques for Experimental-Observation of

Molecular Phenomena Associated with Fracture in Polymers", *Abstracts of Papers of the American Chemical Society*, 1976, 28-28.

19 G. V. Vinogradov, S. E. Sosin and A. I. Elkin, "Fracture of Uncured Linear Flexible-Chain Polymers of Narrow Molecular Mass-Distribution in Triaxial Stress (Behavior of Elastomers as Adhesives)", *Polymer*, 1978, **19**, 1458-1464.

20 H. R. Reese and B. H. Zimm, "Fracture of Polymer-Chains in Extensional Flow - Experiments with DNA, and a Molecular-Dynamics Simulation", *Journal of Chemical Physics*, 1990, **92**, 2650-2662.

21 M. Sambasivam, A. Klein and L. H. Sperling, "The molecular basis of fracture in crosslinked glassy polymers", *Journal of Applied Polymer Science*, 1997, **65**, 1001-1011.

22 H. H. Kausch, J. L. Halary and C. J. G. Plummer, "Crazing and fracture in polymers: Micro-mechanisms and effect of molecular variables", *Macromolecular Symposia*, 2004, **214**, 17-30.

23 H. W. Melville and A. J. R. Murray, "The Ultrasonic Degradation of Polymers", *Transactions of the Faraday Society*, 1950, **46**, 996-1009.

24 P. Baláz, "Mechanical activation in hydrometallurgy", *International Journal of Mineral Processing*, 2003, **72**, 341-354.

25 T. Matsuda, R. Kawakami, T. Nakajima and J. P. Gong, "Crack Tip Field of a Double-Network Gel: Visualization of Covalent Bond Scission through Mechanoradical Polymerization", *Macromolecules*, 2020, **53**, 8787-8795.

26 T. Matsuda, R. Kawakami, R. Namba, T. Nakajima and J. P. Gong, "Mechanoresponsive self-growing hydrogels inspired by muscle training", *Science*, 2019, **363**, 504-508.

27 P. B. Jayathilaka, T. G. Molley, Y. W. Huang, M. S. Islam, M. R. Buche, M. N. Silberstein, J. J. Kruzic and K. A. Kilian, "Force-mediated molecule release from double network hydrogels", *Chemical Communications*, 2021, **57**, 8484-8487.

28 Y. Zheng, J. L. Jiang, M. Jin, D. Miura, F. X. Lu, K. Kubota, T. Nakajima, S. Maeda, H. Ito and J. P. Gong, "In Situ and Real-Time Visualization of

Mechanochemical Damage in Double-Network Hydrogels by Prefluorescent Probe via Oxygen- Relayed Radical Trapping", *Journal of the American Chemical Society*, 2023, **145**, 7376-7389.

29 H. T. Baytekin, B. Baytekin and B. A. Grzybowski, "Mechanoradicals Created in "Polymeric Sponges" Drive Reactions in Aqueous Media", *Angewandte Chemie-International Edition*, 2012, **51**, 3596-3600.

30 K. L. Zhang, J. Huang, W. Zhang, Y. F. Yu, S. B. Deng and G. Yu, "Mechanochemical degradation of tetrabromobisphenol A: Performance, products and pathway", *Journal of Hazardous Materials*, 2012, **243**, 278-285.

31 J. F. Zhou, T. G. Hsu and J. P. Wang, "Mechanochemical Degradation and Recycling of Synthetic Polymers", *Angewandte Chemie-International Edition*, 2023, DOI: 10.1002/anie.202300768.

32 M. H. Abed, I. S. Abbas and H. Canakci, "Influence of mechanochemical activation on the rheological, fresh and mechanical properties of one-part geopolymer grout", *Advances in Cement Research*, 2023, **35**, 96-110.

33 Z. J. Lee, S. C. Tong, T. K. Tang and Y. Y. Lee, "Palm-based cellulose nanofiber isolated from mechano-chemical processing as sustainable rheological modifier in reduced fat mayonnaise", *Journal of Food Science*, 2022, **87**, 3542-3561.

34 J. P. Gong, "Why are double network hydrogels so tough?", *Soft Matter*, 2010, **6**, 2583-2590.

35 Y. H. Na, Y. Tanaka, Y. Kawauchi, H. Furukawa, T. Sumiyoshi, J. P. Gong and Y. Osada, "Necking phenomenon of double-network gels", *Macromolecules*, 2006, **39**, 4641-4645.

36 T. Matsuda, T. Nakajima, Y. Fukuda, W. Hong, T. Sakai, T. Kurokawa, U. Chung and J. P. Gong, "Yielding Criteria of Double Network Hydrogels", *Macromolecules*, 2016, **49**, 1865-1872.

37 T. Nakajima, H. Furukawa, Y. Tanaka, T. Kurokawa, Y. Osada and J. P. Gong, "True Chemical Structure of Double Network Hydrogels", *Macromolecules*, 2009, **42**, 2184-2189.

38 C. Imaoka, T. Nakajima, T. Indei, M. Iwata, W. Hong, A. Marcellan and J. P.

Gong, “Inverse mechanical-swelling coupling of a highly deformed double-network gel”, *Science Advances*, 2023, **9**.

39 S. Ahmed, T. Nakajima, T. Kurokawa, M. A. Haque and J. P. Gong, “Brittle-ductile transition of double network hydrogels: Mechanical balance of two networks as the key factor”, *Polymer*, 2014, **55**, 914-923.

40 R. J. Song, X. Y. Wang, M. Johnson, C. Milne, A. Lesniak-Podsiadlo, Y. H. Li, J. Lyu, Z. S. Li, C. Y. Zhao, L. Z. Yang, I. Lara-Sáez, A. Sigen and W. X. Wang, “Enhanced Strength for Double Network Hydrogel Adhesive Through Cohesion-Adhesion Balance”, *Advanced Functional Materials*, 2024, DOI: 10.1002/adfm.202313322.

41 G. T. Zhang, X. X. Cai, C. Li, J. S. Yao, W. L. Liu, C. D. Qiao, G. D. Li, Q. Wang and J. J. Han, “Construction of Alkaline Gel Polymer Electrolytes with a Double Cross-Linked Network for Flexible Zinc-Air Batteries”, *Acs Applied Polymer Materials*, 2023, **5**, 3622-3631.

42 Q. H. Wu, J. J. Ge, L. Ding and G. C. Zhang, “Unlocking the potentials of gel conformance for water shutoff in fractured reservoirs: Favorable attributes of the double network gel for enhancing oil recovery”, *Petroleum Science*, 2023, **20**, 1005-1017.

43 R. E. Webber, C. Creton, H. R. Brown and J. P. Gong, “Large strain hysteresis and mullins effect of tough double-network hydrogels”, *Macromolecules*, 2007, **40**, 2919-2927.

44 A. Bin Ihsan, T. L. Sun, S. Kuroda, M. A. Haque, T. Kurokawa, T. Nakajima and J. P. Gong, “A phase diagram of neutral polyampholyte - from solution to tough hydrogel”, *Journal of Materials Chemistry B*, 2013, **1**, 4555-4562.

45 K. Hoshino, T. Nakajima, T. Matsuda, T. Sakai and J. P. Gong, “Network elasticity of a model hydrogel as a function of swelling ratio: from shrinking to extreme swelling states”, *Soft Matter*, 2018, **14**, 9693-9701.

46 Q. Chen, H. Chen, L. Zhu and J. Zheng, “Fundamentals of double network hydrogels”, *Journal of Materials Chemistry B*, 2015, **3**, 3654-3676.

47 Z. J. Wang, J. L. Jiang, Q. F. Mu, S. Maeda, T. Nakajima and J. P. Gong, “Azo-

Crosslinked Double-Network Hydrogels Enabling Highly Efficient Mechanoradical Generation", *Journal of the American Chemical Society*, 2022, **144**, 3154-3161.

48 T. Ouchi, B. H. Bowser, T. B. Kouznetsova, X. J. Zheng and S. L. Craig, "Strain-triggered acidification in a double-network hydrogel enabled by multi-functional transduction of molecular mechanochemistry", *Materials Horizons*, 2023, **10**, 585-593.

49 G. M. Wei, Y. Kudo, T. Matsuda, Z. J. Wang, Q. F. Mu, D. R. King, T. Nakajima and J. P. Gong, "Sustainable mechanochemical growth of double-network hydrogels supported by vascular-like perfusion", *Materials Horizons*, 2023, **10**, 4882-4891.

50 Q. F. Mu, K. P. Cui, Z. J. Wang, T. Matsuda, W. Cui, H. Kato, S. Namiki, T. Yamazaki, M. Frauenlob, T. Nonoyama, M. Tsuda, S. Tanaka, T. Nakajima and J. P. Gong, "Force-triggered rapid microstructure growth on hydrogel surface for on-demand functions", *Nature Communications*, 2022, **13**, 6213.

51 J. Slootman, V. Waltz, C. J. Yeh, C. Baumann, R. Gostl, J. Comtet and C. Creton, "Quantifying Rate- and Temperature-Dependent Molecular Damage in Elastomer Fracture", *Physical Review X*, 2020, **10**, 041045.

52 M. Kanik, S. Orguc, G. Varnavides, J. Kim, T. Benavides, D. Gonzalez, T. Akintilo, C. C. Tasan, A. P. Chandrakasan, Y. Fink and P. Anikeeva, "Strain-programmable fiber-based artificial muscle", *Science*, 2019, **365**, 145-150.

53 A. G. Robling and C. H. Turner, "Mechanical Signaling for Bone Modeling and Remodeling", *Critical Reviews in Eukaryotic Gene Expression*, 2009, **19**, 319-338.

54 A. Sharir, T. Stern, C. Rot, R. Shahar and E. Zelzer, "Muscle force regulates bone shaping for optimal load-bearing capacity during embryogenesis", *Development*, 2011, **138**, 3247-3259.

55 H. H. Vandenburgh, "Motion into Mass - How Does Tension Stimulate Muscle Growth", *Medicine and Science in Sports and Exercise*, 1987, **19**, S142-S149.

56 K. M. Tarpenning, R. A. Wiswell, S. A. Hawkins and T. J. Marcell, "Influence

of weight training exercise and modification of hormonal response on skeletal muscle growth", *Journal of Science and Medicine in Sport*, 2001, **4**, 431-446.

57 L. A. Johnson and A. J. Fuglevand, "Mimicking muscle activity with electrical stimulation", *Journal of Neural Engineering*, 2011, **8**, 016009.

58 A. M. Kasper, D. C. Turner, N. R. W. Martin and A. P. Sharples, "Mimicking exercise in three-dimensional bioengineered skeletal muscle to investigate cellular and molecular mechanisms of physiological adaptation", *Journal of Cellular Physiology*, 2018, **233**, 1985-1998.

59 S. Lv, D. M. Dudek, Y. Cao, M. M. Balamurali, J. Gosline and H. B. Li, "Designed biomaterials to mimic the mechanical properties of muscles", *Nature*, 2010, **465**, 69-73.

60 H. E. H. Meijer and L. E. Govaert, "Mechanical performance of polymer systems: The relation between structure and properties", *Progress in Polymer Science*, 2005, **30**, 915-938.

61 Y. J. Che, D. P. Li, Y. L. Liu, Q. L. Ma, Y. B. Tan, Q. Y. Yue and F. J. Meng, "Physically cross-linked pH-responsive chitosan-based hydrogels with enhanced mechanical performance for controlled drug delivery", *Rsc Advances*, 2016, **6**, 106035-106045.

62 Z. T. Bao, C. H. Xian, Q. J. Yuan, G. T. Liu and J. Wu, "Natural Polymer-Based Hydrogels with Enhanced Mechanical Performances: Preparation, Structure, and Property", *Advanced Healthcare Materials*, 2019, **8**, 1900670.

63 A. Dutta, K. Ghosal, K. Sarkar, D. Pradhan and R. K. Das, "From ultrastiff to soft materials: Exploiting dynamic metal-ligand cross-links to access polymer hydrogels combining customized mechanical performance and tailorable functions by controlling hydrogel mechanics", *Chemical Engineering Journal*, 2021, **419**, 129528.

64 T. Nonoyama and J. P. Gong, "Double-network hydrogel and its potential biomedical application: A review", *Proceedings of the Institution of Mechanical Engineers Part H-Journal of Engineering in Medicine*, 2015, **229**, 853-863.

65 A. Nakayama, A. Kakugo, J. P. Gong, Y. Osada, M. Takai, T. Erata and S.

Kawano, “High mechanical strength double-network hydrogel with bacterial cellulose”, *Advanced Functional Materials*, 2004, **14**, 1124-1128.

66 G. J. Laurent, M. P. Sparrow, P. C. Bates and D. J. Millward, “Turnover of Muscle Protein in Fowl - Collagen Content and Turnover in Cardiac and Skeletal-Muscles of Adult Fowl and Changes during Stretch-Induced Growth”, *Biochemical Journal*, 1978, **176**, 419-427.

67 C. W. Kang, M. L. Sunde and R. W. Swick, “Growth and Protein-Turnover in the Skeletal-Muscles of Broiler Chicks”, *Poultry Science*, 1985, **64**, 370-379.

68 D. M. Skjaerlund, D. R. Mulvaney, W. G. Bergen and R. A. Merkel, “Skeletal-Muscle Growth and Protein-Turnover in Neonatal Boars and Barrows”, *Journal of Animal Science*, 1994, **72**, 315-321.

69 N. Park and J. Kim, “Hydrogel-Based Artificial Muscles: Overview and Recent Progress”, *Advanced Intelligent Systems*, 2020, **2**, 1900135.

70 E. Ducrot, Y. L. Chen, M. Bulters, R. P. Sijbesma and C. Creton, “Toughening Elastomers with Sacrificial Bonds and Watching Them Break”, *Science*, 2014, **344**, 186-189.

71 B. De Rybel, M. Adibi, A. S. Breda, J. R. Wendrich, M. E. Smit, O. Novák, N. Yamaguchi, S. Yoshida, G. Van Isterdael, J. Palovaara, B. Nijsse, M. V. Boekschoten, G. Hooiveld, T. Beeckman, D. Wagner, K. Ljung, C. Fleck and D. Weijers, “Plant developement Integration of growth and patterning during vascular tissue formation in Arabidopsis”, *Science*, 2014, **345**, 1255215.

72 J. H. Jung and C. M. Park, “Vascular development in plants: Specification of xylem and phloem tissues”, *Journal of Plant Biology*, 2007, **50**, 301-305.

73 H. Fukuda and K. Ohashi-Ito, “Vascular tissue development in plants”, *Plant Development and Evolution*, 2019, **131**, 141-160.

74 J. S. Miller, K. R. Stevens, M. T. Yang, B. M. Baker, D. H. T. Nguyen, D. M. Cohen, E. Toro, A. A. Chen, P. A. Galie, X. Yu, R. Chaturvedi, S. N. Bhatia and C. S. Chen, “Rapid casting of patterned vascular networks for perfusable engineered three-dimensional tissues”, *Nature Materials*, 2012, **11**, 768-774.

75 P. S. Hwang and D. S. Willoughby, “Mechanisms Behind Blood Flow-

Restricted Training and Its Effect toward Muscle Growth", *Journal of Strength and Conditioning Research*, 2019, **33**, S167-S179.

76 A. R. Hamilton, N. R. Sottos and S. R. White, "Self-Healing of Internal Damage in Synthetic Vascular Materials", *Advanced Materials*, 2010, **22**, 5159-5163.

77 E. N. Brown, N. R. Sottos and S. R. White, "Fracture testing of a self-healing polymer composite", *Experimental Mechanics*, 2002, **42**, 372-379.

78 E. N. Brown, S. R. White and N. R. Sottos, "Microcapsule induced toughening in a self-healing polymer composite", *Journal of Materials Science*, 2004, **39**, 1703-1710.

79 N. Sottos, S. White and I. Bond, "Introduction: self-healing polymers and composites", *Journal of the Royal Society Interface*, 2007, **4**, 347-348.

80 S. R. White, B. J. Blaiszik, S. L. B. Kramer, S. C. Olugebefola, J. S. Moore and N. R. Sottos, "Self-healing Polymers and Composites", *American Scientist*, 2011, **99**, 392-399.

81 G. Fridman, M. Peddinghaus, H. Ayan, A. Fridman, M. Balasubramanian, A. Gutsol, A. Brooks and G. Friedman, "Blood coagulation and living tissue sterilization by floating-electrode dielectric barrier discharge in air", *Plasma Chemistry and Plasma Processing*, 2006, **26**, 425-442.

82 S. Wang, H. K. Beech, B. H. Bowser, T. B. Kouznetsova, B. D. Olsen, M. Rubinstein and S. L. Craig, "Mechanism Dictates Mechanics: A Molecular Substituent Effect in the Macroscopic Fracture of a Covalent Polymer Network", *Journal of the American Chemical Society*, 2021, **143**, 3714-3718.

83 C. Baumann, M. Stratigaki, S. P. Centeno and R. Göstl, "Multicolor Mechanofluorophores for the Quantitative Detection of Covalent Bond Scission in Polymers", *Angewandte Chemie-International Edition*, 2021, **60**, 13287-13293.

84 J. N. M. Boots, D. W. te Brake, J. M. Clough, J. Tauber, J. Ruiz-Franco, T. E. Kodger and J. van der Gucht, "Quantifying bond rupture during indentation fracture of soft polymer networks using molecular mechanophores", *Physical Review Materials*, 2022, **6**, 025605.

85 J. Taipale and J. KeskiOja, “Growth factors in the extracellular matrix”, *Faseb Journal*, 1997, **11**, 51-59.

86 N. K. Karamanos, A. D. Theocharis, Z. Piperigkou, D. Manou, A. Passi, S. S. Skandalis, D. H. Vynios, V. Orian-Rousseau, S. Ricard-Blum, C. E. H. Schmelzer, L. Duca, M. Durbee, N. A. Afratis, L. Troeberg, M. Franchi, V. Masola and M. Onisto, “A guide to the composition and functions of the extracellular matrix”, *Febs Journal*, 2021, **288**, 6850-6912.

87 S. L. K. Bowers, I. Banerjee and T. A. Baudino, “The extracellular matrix: At the center of it all”, *Journal of Molecular and Cellular Cardiology*, 2010, **48**, 474-482.

88 F. T. Bosman and I. Stamenkovic, “Functional structure and composition of the extracellular matrix”, *Journal of Pathology*, 2003, **200**, 423-428.

89 C. Frantz, K. M. Stewart and V. M. Weaver, “The extracellular matrix at a glance”, *Journal of Cell Science*, 2010, **123**, 4195-4200.

90 K. Afshar, M. J. Sanaei, M. S. Ravari, A. Pourbagheri-Sigaroodi and D. Bashash, “An overview of extracellular matrix and its remodeling in the development of cancer and metastasis with a glance at therapeutic approaches”, *Cell Biochemistry and Function*, 2023, **41**, 930-952.

Chapter 3 Channel Structures in DN Gel

3.1. Introduction

How to integrate vascular structures into a matrix is the first step of consideration. Many methods that are commonly used in lab chip studies have been adapted to structural hydrogel studies, such as photolithography,[1-3] replica molding and sacrificial templates assisted soft lithography.[4] Specifically, for the complex 3D channels that is non-planar in geometry, it is more easy and promising to make a degradable mold beforehand.[5] The mold serves as a versatile sacrificial template, which is supposed to leave the channeled trajectory in the matrix after removal. Although years have passed, the method of utilizing sacrificial molds still plays an important role in building up structures in soft materials.[6-11]

In this chapter, we used capillary tube as a sacrificial mold to construct a channel inside the DN gel matrix, after connected the channel with tubes, solution is able to perfuse the DN gel through the vascular-like channel. Diffusion through the channel was measured by ATR-FTIR signals.

We proved the feasibility of using the channel-structured DN gel as the structural bases to support monomers delivering through vascular-like channels. Works in this chapter function as the preparation for the following attempts of using channel as the supply path for monomers and crosslinkers, therefore sustaining the mechanoradical polymerization in DN gel.

3.2. Experiments

3.2.1. Materials

2-Acrylamido-2-methylpropane sulfonic acid sodium salt (NaAMPS, 49.8 wt. % aqueous solution) was provided by Toagosei. Acrylamide (AAm) was purchased from Junsei Chemical. N,N'-Methylenebisacrylamide (MBAA), ultraviolet (UV) initiator a-ketoglutaric acid (a-keto), N-isopropylacrylamide (NIPAAm), and neutral red were purchased from Wako Pure Chemical Industries. All the reagents were used as received.

3.2.2. 3D Printed Capillary Tube Mold

Glass capillary tubes were used as the sacrificial mold during the curing process of the PNaAMPS hydrogel (first network). In order to fix the capillaries in the middle of the curing chamber, a square shaped mold: 8 cm × 8 cm (width × length) as shown in **Figure 3.1** is 3D printed using a 3D printer (AGILISTA-3000, Keyence), capillaries with outer diameter of 0.5 mm were used to inserted into the mold.

3.2.3. Synthesis of PNaAMPS Gel with Channel

The internal channel of the DN hydrogel was fabricated using a glass capillary tube as the sacrificial mold. The 3d printed mold was used to fix the capillary tubes in the middle of the chamber, then sandwiched in two 10 cm × 10 cm glass plates and sealed with silicone sheet, using this setups to keep the capillary in the center of the gel **(Figure 3.2)**. Finally, the precursor aqueous solution of the first-network containing NaAMPS (1 M), MBAA (2.5 mol% with respect to the monomer), and 2-oxoglutaric acid (1.0 mol% with respect to the monomer) were poured into the mold and irradiated under UV light for 9 h in an Ar atmosphere. The gel of the first network was cut into pieces

with a capillary in the middle and then immersed in the second network precursor. As the polyelectrolyte hydrogel swells during this process, the channel becomes wider so the capillary can be easily removed and leave a channel inside.

3.2.4. Synthesis of Channel-Integrated Double-Network (c-DN) Hydrogel

The PNaAMPS hydrogel was then laser-cut into rectangular pieces with a capillary in the middle, and immersed in the precursor aqueous solution of the second network gel containing AAm (3 M), MBAA (0.01 mol%), and 2-oxoglutaric acid (0.01 mol%). After the PNaAMPS gels reached the swelling equilibrium, the channel was almost three times wider in diameter. Consequently, the capillaries can be easily removed. Then, we used high-pressure air to blow away the solutions inside the channel and inserted another capillary tube (1.4 mm) to maintain the channel shape. Finally, the gel was sandwiched between two glass plates and irradiated with UV light for 9 h in an Ar atmosphere to synthesize the second PAAm network. The DN gels were then immersed in a large volume of water to remove unreacted reagents.

3.2.5. Diffusion Measurement Using ATR FT-IR

The absorbance signal of monomers diffusing from the channel to the surface of c-DN gels was detected by an ATR-FTIR spectrometer (FT-IR 6600, Jasco corporation). For measuring the calibration, DN gel slices with the same constitution to the c-DN hydrogel sample were soaked in standard monomer solutions for 2 days. The calibration results of NIPAAm and NaAMPS were used to calculate the monomer concentration change during the circulatory flow. To detect the diffusion kinetics of monomer solution, 0.1 M NaAMPS and 1.0 M NIPAAm solutions were used to perfuse the c-DN hydrogel through the internal channel, The liquid circulation speed was set at 0.13 mL s^{-1}. The

gauge part of the c-DN hydrogel was fixed on the measurement substrate with a close contact to the ATR-IR crystal, signals were collected from the outer surface of the c-DN gel.

3.3. Results and Discussion

3.3.1. c-DN Gel and Circulatory System

Photographs of the c-DN gel are shown in **Figure 3.3a**. A channel with a diameter of 1.6 mm was located at the center of the gauge and evenly crossed through the sample from one side to the other. To connect the channel of the c-DN gel to the circulation system, the two ends of the channel were connected to flexible tubes using Luer-locks. Owing to the elastic and tough properties of the c-DN gel, no liquid leakage occurred when the c-DN gel was subjected to deformations, such as twisting or bending (**Figure 3.3b**). To place the c-DN gel in the tensile machine, the two clamping regions were fixed using specially designed jigs (**Figure 3.4**). This setup enabled liquids to flow in the channel during cyclic tensile loading. As shown in **Figure 3.5**, the channel in the c-DN hydrogel functioned perfectly as a liquid-delivery pathway during tensile tests.

3.3.2. Diffusion Through the Vascular-Like Channel

As a permeable substance, the c-DN hydrogel allowed the diffusion of chemicals from the channel into the gel matrix. ATR-FTIR signals were collected from the outer surface of the c-DN gel, the calibration results of NaAMPS (**Figure 3.6**) and NIPAAm (**Figure 3.7**) were used to calculate the monomer concentration change during the circulatory flow. For NIPAAm, the symmetrical deformation vibration absorption peaks of the isopropyl group located at 1371 and 1388 cm^{-1} were monitored.[12] With the circulation of a 1 M NIPAAm aqueous solution, the NIPAAm concentration at the outer surface

gradually increased with time and eventually saturated in 90 min. A similar saturation time (~90 minutes) was observed with the circulation of 0.1 M NaAMPS, where the signal of the characteristic asymmetric stretching of sulfonic group peak ($\nu_{S=O}$) of NaAMPS at 1043 cm^{-1} was monitored.[13-15] These results show that the two monomers diffused into the DN gels and reached an equilibrium concentration at ~90 min. In addition, the perfusion of aqueous solutions through the channel can replenish the water loss and prevent drying, which solves the problem of hydrogels in the air due to the surface evaporation of water.[16] This is demonstrated by the long-term cyclic tensile tests of the c-DN gel in the air at room temperature (**Figure 3.8**). Without water circulation, the c-DN gel gradually dehydrated and became brittle, and eventually fractured within 2 h, whereas the gel with water circulation remained moist and soft, even after 12 h of cyclic tensile testing, indicating that the c-DN gel maintained a stable water content. Hence, vascular-like perfusion not only replenishes chemicals but also water, which paves the way for continuous self-strengthening in a dry environment through hours of cyclic mechanical training.

3.4. Conclusions

We constructed a channel inside DN hydrogel using the capillary tubes as sacrificial mold, the dimension of the sacrificial mold and the resulted internal channel is illustrated. Besides, the c-DN gel can be connected to an external circulation system for a vascular-like perfusion through the inner channel, we present the results of solution flowing inside the c-DN hydrogel even during deformations such as stretching, bending and twisting. Besides, the continuous internal circulation of liquid is demonstrated to proficiently supplement the evaporative loss of moisture from the gel, thereby preserving the moisture and softness of the c-DN hydrogel in ambient conditions,

guaranteeing their pliable characteristics and exhibiting a stable mechanical property during extended cyclic tensile tests. To determine the diffusion of monomer molecules from the internal channel wall to the outer surface of c-DN hydrogel, the chemical signals of monomers is measured, hence the time required for a thoroughly penetration of the monomer solution into the hydrogel is preliminarily determined.

Figures

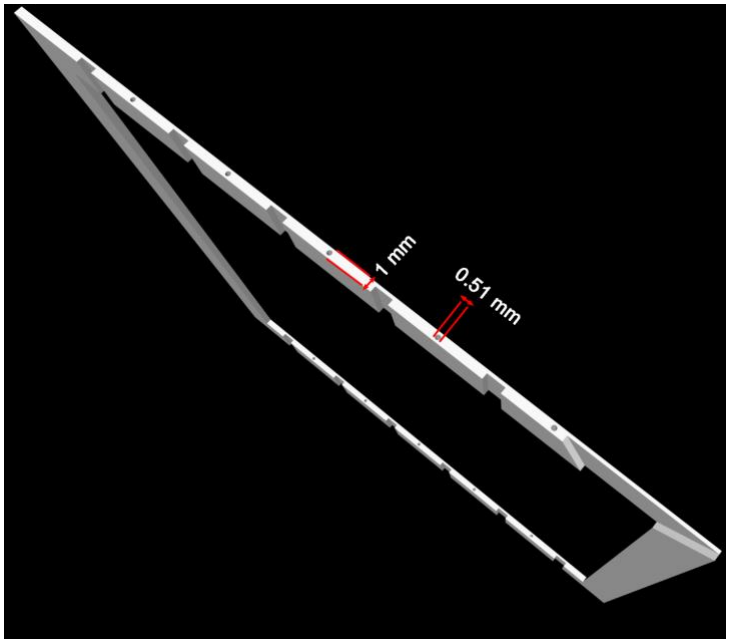


Figure 3.1. The square shaped mold: 8 cm×8 cm (wide×length) for fixing capillaries during the curing process of the PNaAMPS hydrogel (first network).

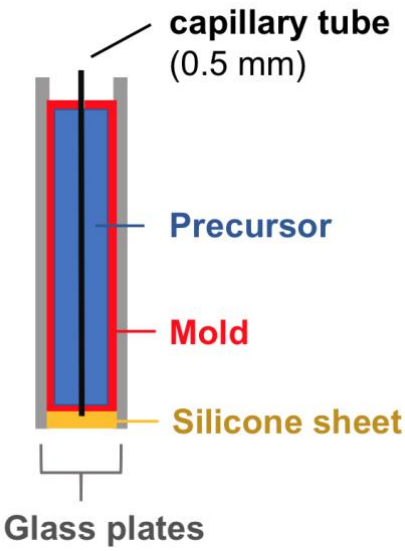


Figure 3.2. Side view of synthesized PNaAMPS gel with a channel in the middle.

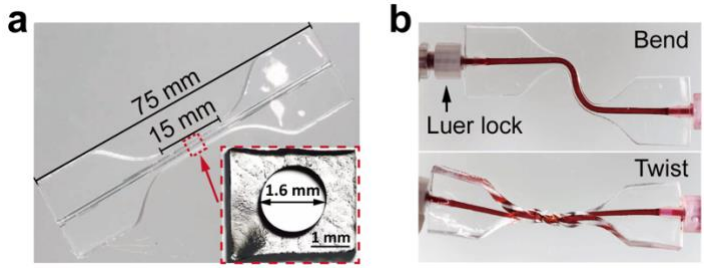


Figure 3.3. (a) Photograph of the fabricated c-DN gel in dumbbell shape for cyclic tensile loading. The insert photo shows the cross-sectional photo of the gel in gauge region, as indicated by an arrow. (b) Photos of the c-DN gel under bending and twisting without leakage of the flowing liquid (dyed in red).

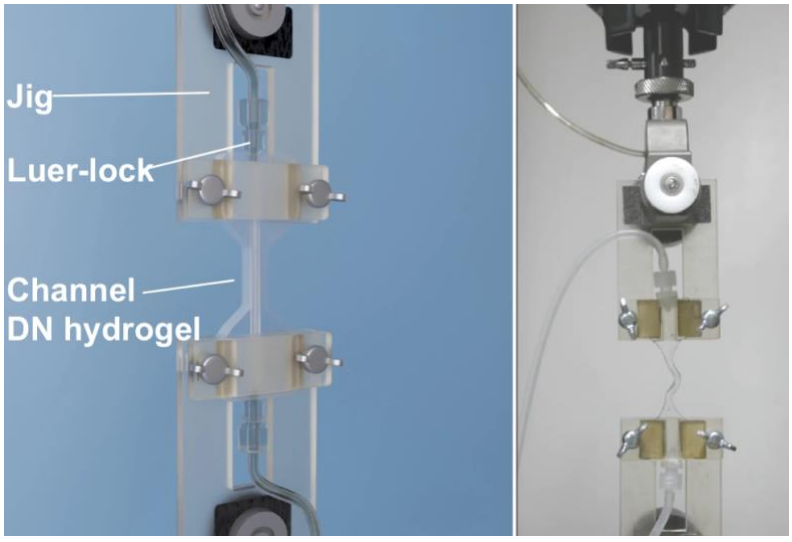


Figure 3.4. Setup for tensile test of c-DN gel with specially designed jigs enabling liquid flow through the channel during stretching.

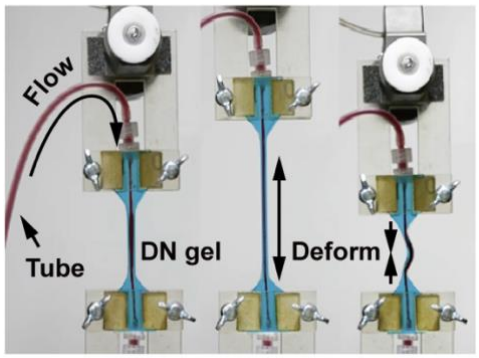


Figure 3.5. Photos of c-DN gel (dyed in blue) during tensile test with flowing liquid (dyed in red).

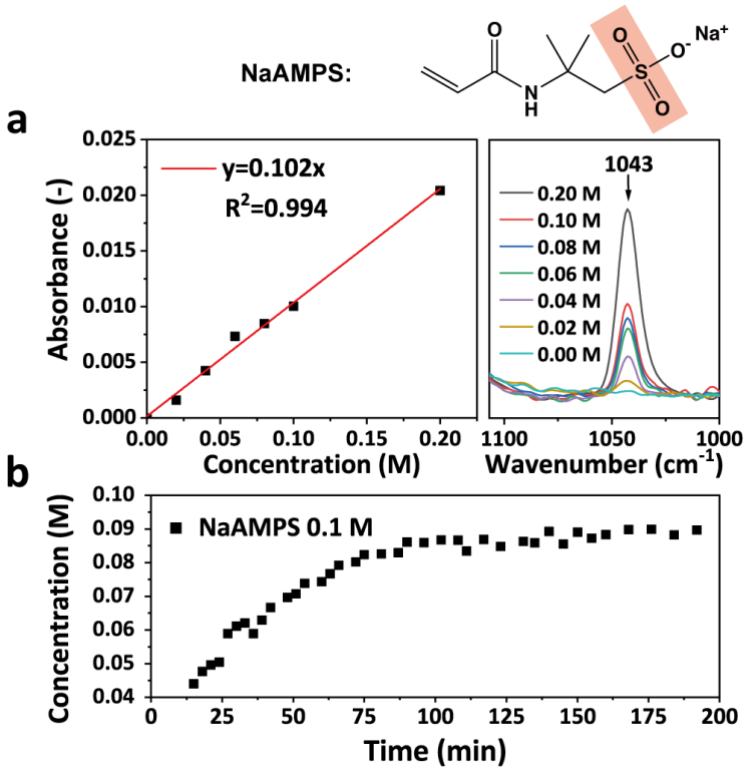


Figure 3.6. ATR-FTIR spectra results of NaAMPS. **a.** Absorbance collected from peak of 1043 cm^{-1}, spectra were taken from DN hydrogels after soaked in 0.20, 0.10, 0.08, 0.06, 0.04, 0.02, and 0.00 M standard NaAMPS solutions. **b.** Time profile of concentration of NaAMPS on the surface of c-DN gel (0.8 mm from the circular channel surface) during circulation of the 0.1 M NaAMPS aqueous solution.

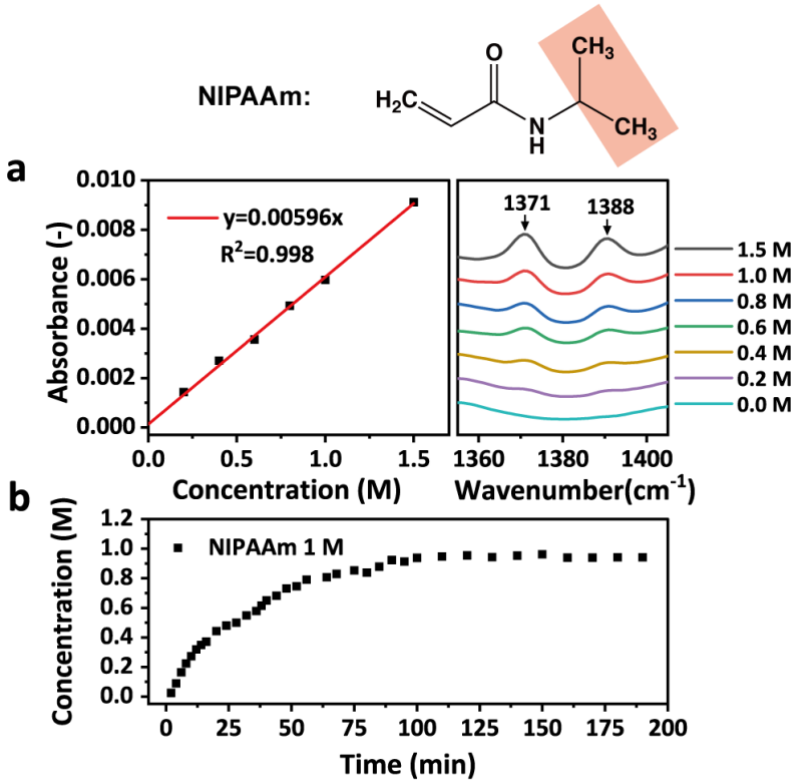


Figure 3.7. ATR-FTIR results of NIPAAm. **a.** Absorbance collected from peak of 1371 cm^{-1}, spectra were taken from DN hydrogels after soaked in 1.5, 1.0, 0.8, 0.6, 0.4, 0.2, and 0 M standard NIPAAm solutions. **b.** Time profile of concentration of NIPAAm on the surface of c-DN gel (0.8 mm from the circular channel surface) during circulation of 1.0 M NIPAAm aqueous solution.

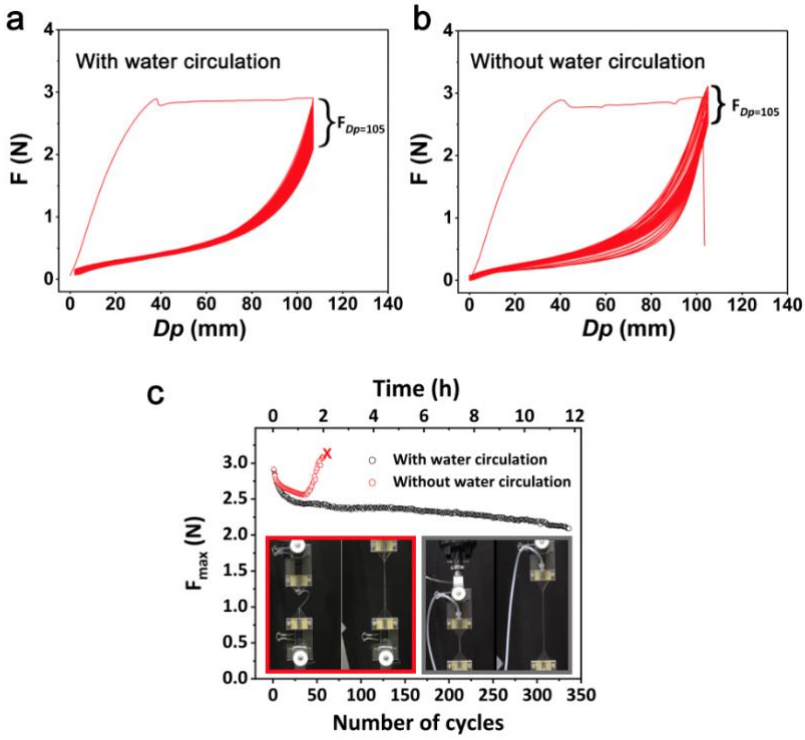


Figure 3.8. Stability of c-DN hydrogel in open air illustrated by cyclic tensile tests. **a.** With, and **b.** Without continuous water circulation. **c.** Tensile force at a displacement (*Dp*) of 105 mm for the upper jig as a function of cyclic number and time. The inserted images depict the final sample appearances without water circulation (red frame, dry and brittle after 2 h) and with continuous water circulation (black frame, moist and soft after 12 h).

3.5. Reference

1 K. T. M. Tran and T. D. Nguyen, “Lithography-based methods to manufacture biomaterials at small scales”, *Journal of Science-Advanced Materials and Devices*, 2017, **2**, 1-14.

2 A. Aazmi, H. Z. Zhou, Y. T. Li, M. F. Yu, X. B. Xu, Y. T. Wu, L. Ma, B. Zhang and H. Y. Yang, “Engineered Vasculature for Organ-on-a-Chip Systems”, *Engineering*, 2022, **9**, 131-147.

3 J. Tam and O. Yasar, “Multi Material 3D Scaffold Printing with Maskless Photolithography”, *Mrs Advances*, 2017, **2**, 1303-1308.

4 S. F. Lyuksyutov, R. A. Vaia, P. B. Paramonov, S. Juhl, L. Waterhouse, R. M. Ralich, G. Sigalov and E. Sancaktar, “Electrostatic nanolithography in polymers using atomic force microscopy”, *Nature Materials*, 2003, **2**, 468-472.

5 J. S. Miller, K. R. Stevens, M. T. Yang, B. M. Baker, D. H. T. Nguyen, D. M. Cohen, E. Toro, A. A. Chen, P. A. Galie, X. Yu, R. Chaturvedi, S. N. Bhatia and C. S. Chen, “Rapid casting of patterned vascular networks for perfusable engineered three-dimensional tissues”, *Nature Materials*, 2012, **11**, 768-774.

6 L. M. Bellan, S. P. Singh, P. W. Henderson, T. J. Porri, H. G. Craighead and J. A. Spector, “Fabrication of an artificial 3-dimensional vascular network using sacrificial sugar structures”, *Soft Matter*, 2009, **5**, 1354-1357.

7 M. K. Gelber and R. Bhargava, “Monolithic multilayer microfluidics sacrificial molding of 3D-printed isomalt”, *Lab on a Chip*, 2015, **15**, 1736-1741.

8 W. L. Tang, H. Liu, L. Y. Zhu, J. P. Shi, Z. A. Li, N. Xiang and J. Q. Yang, “Fabrication of Different Microchannels by Adjusting the Extrusion Parameters for Sacrificial Molds”, *Micromachines*, 2019, **10**, 10080544.

9 E. Davoodi, H. Montazerian, A. Khademhosseini and E. Toyserkani, “Sacrificial 3D printing of shrinkable silicone elastomers for enhanced feature resolution in flexible tissue scaffolds”, *Acta Biomaterialia*, 2020, **117**, 261-272.

10 W. H. Goh and M. Hashimoto, “Dual Sacrificial Molding: Fabricating 3D Microchannels with Overhang and Helical Features”, *Micromachines*, 2018, **9**,

9100523.

11 N. Ferrell, J. Woodard and D. Hansford, “Fabrication of polymer microstructures for MEMS: sacrificial layer micromolding and patterned substrate micromolding”, *Biomedical Microdevices*, 2007, **9**, 815-821.

12 D. Lin-Vien, N. B. Colthup, W. G. Fateley and J. G. Grasselli, *The Handbook of Infrared and Raman Characteristic Frequencies of Organic Molecules*, Academic Press, 1991.

13 N. Devi and A. Narzary, “Release Dynamics of Brufen from a Drug-Loaded Polymer Hydrogel Containing Polyvinyl Alcohol, 2-Acrylamide-2-methylpropane Sulfonic Acid and Acrylamide”, *International Journal of Polymeric Materials*, 2012, **61**, 821-833.

14 A. Selvarajan, “Raman spectrum of dimethyl sulfoxide (DMSO) and the influence of solvents”, *Proceedings of the Indian Academy of Sciences - Section A*, 1966, **64**, 44–50.

15 D. S. Warren and A. J. McQuillan, “Infrared spectroscopic and DFT vibrational mode study of perfluoro(2-ethoxyethane) sulfonic acid (PES), a model Nafion side-chain molecule”, *Journal of Physical Chemistry B*, 2008, **112**, 10535-10543.

16 Y. Sekine and T. Ikeda-Fukazawa, “Structural changes of water in a hydrogel during dehydration”, *Journal of Chemical Physics*, 2009, **130**, 034501.

Chapter 4 Mechanoradical Polymerization in c-DN Gel

4.1. Introduction

Based on the principle that the cleavage of bonds in the brittle first network will generate chain-end radicals,[1-4] we are able to initiated the pre-loaded monomers in the DN gel, and polymerize new polymers by applying external forces to the DN gel.[5] The mechanical energy applied to DN gels is efficiently transferred to the chemical bonds of the brittle network,[6] generating mechanoradicals that initiate the polymerization of pre-loaded monomers, thereby remodeling the materials in-situ.

4.2. Experiments

4.2.1. Materials

Ammonium iron(II) sulfate ($(NH_4)_2FeII(SO_4)_2$) hexahydrate, sulfuric acid (H_2SO_4), N-isopropylacrylamide (NIPAAm), 2-oxoglutaric acid, xylenol orange (XO), and neutral red were purchased from Wako Pure Chemical Industries. 8-Anilino-1-naphthalenesulfonic acid (ANS) was purchased from Tokyo Chemical Industry. All the reagents were used as received.

4.2.2. Evaluation of Mechanoradical Concentration by Fenton Color Reaction

The mechanoradical concentration in c-DN gels was determined by a method reported in our previous work.[7] c-DN hydrogels were immersed in an aqueous solution of 100 μM $(NH4)_2Fe^{II}(SO_4)_2$, 100 μM XO and 20 mM H_2SO_4 for 1 day. Then gels were stretched to the preset strain (ε_{max} = 7) at a velocity of 100 mm min^{-1} and then immediately recovered to the initial position. After 30 mins, when no further color

change was observed, the gels were cut with scissors to obtain the gauge part, which was then placed in a quartz optical cell (45 mm × 10 mm × 10 mm) for UV-visible absorption spectroscopy (UV-1800, Shimadzu Co.) measurement. To quantify the Fe^{3+} concentration, the calibration of our former work was used as the constitution is the same.[7] By comparing the normalized absorbance at 580 nm of DN gels after stretching with the calibration curve, we can evaluate the Fe^{3+} concentration, which is assumed to be equal to the mechanoradical concentration.[3, 8, 9]

4.2.3. Preparation of fluorescence spectroscopy sample

All the samples and solutions got deoxygenated in argon atmosphere for 24 hours. For the pre-flow group, the stretch and flow protocol is shown in **Figure 4.1**, the c-DN hydrogel got perfused through the channel by a circulatory flow of 1.0 M NIPAAm aqueous solution before tensile tests. After various of pre-flow times of 2, 5, 10, 15, 30, 60, and 90 minuets, we stopped the flow and drained the solution in the channel by Argon air flow, the gel was then loaded to a strain of 7, at which state the gel was fully yielded, and then got unloaded to its original state of unstretched. After the tensile stretch was released, the sample was immediately exposed to open air to quench the polymerization.

For the post-flow group as shown in **Figure 4.2**, we load-unload the gel first, and then circulate the NIPAAm solution for 90 minuets. Both pre-flow and post-flow groups got stretched at 15 °C controlled by the temperature conditioner in the glove box. And after unloading the samples, the gauge part were all got cut immediately in order to prevent further diffusion. The samples were then soaked in 200 mg L^{-1} ANS aqueous solution and stored below 10 °C for 1 day before the LSCM observation. The crosshead velocity of the load-unload process is both 300 mm min^{-1}.

4.2.4. Fluorescence observation using LSCM

A laser scanning confocal microscope (Nikon A1 Rsi and Ti-E, Nikon Co.) was used to observe the in situ mechanoradical polymerization of NIPAAm. The sample temperature (45 °C) was adjusted using a stage-top incubator (INUBG2H-TIZB, Tokai Hit Co.). We used a Plan Fluor × 4 objective lens (NA 0.13, Nikon Co.) and set the excitation laser wavelength to 402.5 nm. For quantification purposes, the fluorescence emission for all measurements was set in the wavelength range of 425–475 nm under the same laser intensity.

4.3. Results and Discussion

4.3.1. Mechanoradical Concentration of c-DN gels

The mechanism of Fenton color reaction induced by mechanoradicals is shown in **Figure 4.3 a,** optical images of the Fenton color reaction in a c-DN hydrogel induced by mechanoradicals is shown in **Figure 4.3 b**, the channel will not influence the mechanoradical generation and an color change that is characteristic of the presence of Fe^{3+} was observed in the necked region. By the UV-visible spectra of the stretched gels in **Figure 4.3 c**, we can evaluate the Fe^{3+} concentration. Assuming that all types of mechanoradicals generated by bond scission have the same reactivity in the Fenton solution, the mechanoradical concentration in the completely necked DN gel was estimated to be on the order of 10^{-5} M.

4.3.2. Diffusion-Limited Mechanoradical Polymerization

For visualizing mechanoradical polymerization profiles of the stretched c-DN gels, we adopted NIPAAm as the monomer that perfused in the channel, as illustrated in **Figure**

4.4, after a pre-set time of the vascular-like flow of NIPAAm monomer, a stretch was applied and the mechanoradicals initiate an in-situ polymerization and forms poly-NIPAM chains. These newly formed polymers become hydrophobic after heating, and we used ANS, which is a reagent that fluoresces in hydrophobic environments, to indicate the area with in-situ polymerized NIPAAM.[10-12] The fluorescence mechanism is shown in **Figure 4.5**, by elevating the temperature above the lowest critical solution temperature (LCST) of PNIPAAm (~32 °C), the newly formed PNIPAAm became hydrophobic and underwent a coil–globule transition.[13, 14] As a result, the diffusion area becomes clearly visible under the confocal microscope.

As shown in **Figure 4.6 a**, green fluorescence was observed in all the stretched samples after perfusion with the NIPAAm aqueous solution, indicating the formation of PNIPAAm by in situ mechanoradical polymerization . The fluorescent area developed from the channel wall towards the outer surface with increasing circulation time and eventually reached a spatially uniform distribution in 90 min.

Because the mechanical damage to the gel by tensile deformation was almost uniform in the sample, the fluorescence distribution corresponded to the concentration distribution of NIPAAm at different circulation times. **Figure 4.6 b** shows the fluorescence intensity distributions along the diagonal direction (as indicated by the white line in the 90 min sample in **Figure 4.6 a** for different durations of circulation. An intensity gradient from the center to the outer surface was observed even when the diffusion time was only 2 min, owing to the high monomer concentration gradient at the beginning of circulation. After 90 min of circulation, the fluorescence intensity finally became homogeneous.

4.3.3. Life-time of Mechanoradicals

A post-flow experiment was designed to surmise the duration of mechanoradicals generated in DN hydrogel. As shown in **Figure 4.2**, we applied a stretch before NIPAAm solution circulation, which means that the diffusion from the channel flow was started just after the mechanoradical generation triggered by the force, and the post-flow was set to be 90 minutes to ensure that the hydrogel got fully saturated with monomer eventually. The LSCM image of the post-flow sample is shown in **Figure 4.7 a**, very interestingly, strong fluorescence intensity was observed around the channel, which corresponds to a polymerized zone of PNIPAAm similar to the sample that got pre-flow for a short time. These results imply that the mechanoradicals generated by deformation of a c-DN hydrogel would keep ability to initiate polymerization of monomers diffusing into the gel for a certain period. Unique long lifetime of mechanoradicals may be because of the low-mobility of the chain-end radicals fixed on the network,[15-22] which leads formation of PNIPAAm polymerized zone around the channel. While monomers diffusing from the channel to the c-DN hydrogel, the possibility of activated mechanoradicals to meet their destiny monomers during their limited lifetime becomes lower with increasing distance from the channel wall. Consequently, only the areas around the channel would form significant amount of PNIPAAm strands, which also present us with the time scale of mechanoradicals existence.

A comparison of the profile with the pre-diffusion ones shows that the obtained post-diffusion profile is close to the pre-diffusion result with 10 min circulation (**Figure 4.7 b**). This suggests that a characteristic lifetime of the mechanoradicals in the deformed c-DN hydrogel might be around 10 min. Although diffusion continues after 10 min, there exhibit negligible fluorescence in the area away from the centre of the c-

DN hydrogel that need more time to saturate with monomers.

4.4. Conclusions

Analogous to biological activities supported by the circulatory system, the channel in c-DN gel functions as a delivering pathway for monomer solutions, resulting in a diffusion limited mechanoradical polymerization. Such limited in-situ mechanoradical polymerization was visualized by a hydrophobic fluorescent reagent. Moreover, taking advantage of the visualized diffusion process, we established a reference of diffusion time scale, the caliber of diffusion provided us a facile method to estimate the lifetime of mechanoradicals. Because the monomer diffusion and mechanoradical polymerization share the same time scale, we can therefore decipher the lifetime of mechanoradicals from the diffusion area around the channel, still this mechanoradical life-time should be further investigated and confirmed in subsequent studies.

While in situ reactions in polymer matrices are drawing more attention from researchers,[23, 24] these results verify that the c-DN gel can be adopted as a long-term mechano- radical system working in a dry environment.

Figures

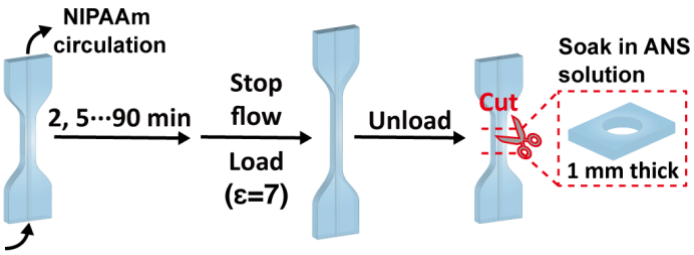


Figure 4.1. Illustration of the protocol to prepare the pre-flow samples, a tensile stretch is applied after a preset circulation time.

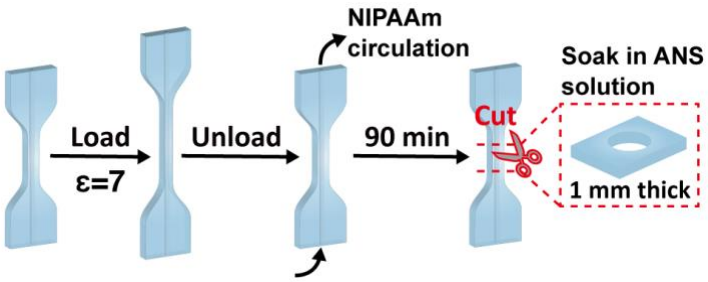
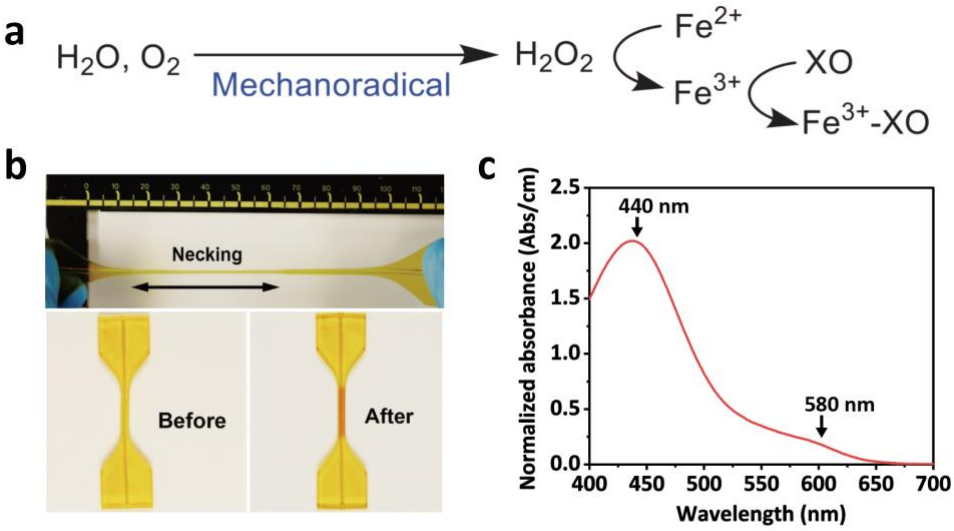


Figure 4.2. Illustration of the protocol to prepare the post-flow samples, a tensile stretch is applied before NIPAAm circulation.



	A_{580}/A_{440}	$[Fe^{3+}]$ (μM)
c-DN hydrogel	0.1224	16.40

Figure 4.3. Quantification of Fe^{2+} oxidation in a stretched c-DN hydrogel based on the Fenton reaction. **a.** Fenton color reaction induced by mechanoradicals. **b.** Optical images of the Fenton color reaction in a c-DN hydrogel induced by mechanoradicals, an aqueous solution of 100 μM $(NH_4)_2Fe^{II}(SO_4)_2$, 250 μM XO and 20 mM H_2SO_4 was used to emphasize the color contrast. **c.** The UV-visible spectra of the stretched gels fed with ferrous ions and XO. The chart underneath reveals the calculation results.

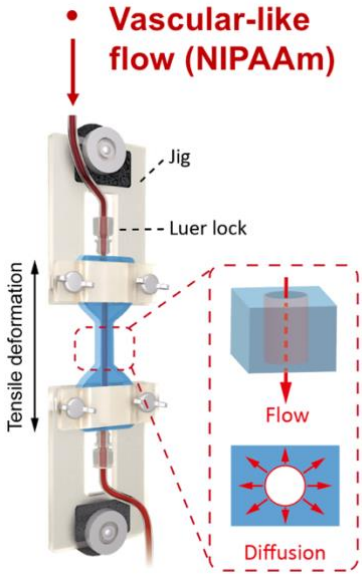


Figure 4.4. Vascular flow of NIPAAM monomer solution in the channel

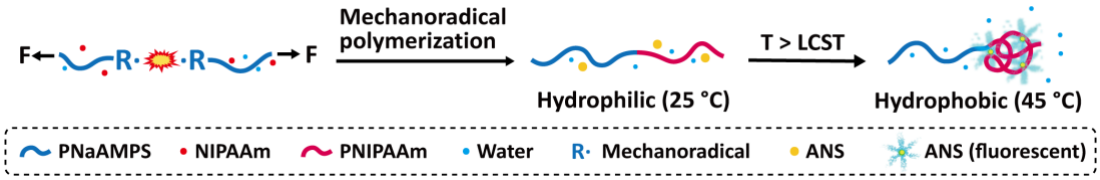


Figure 4.5. Fluorescence mechanism of the prestretched DN hydrogel fed by NIPAAm, the mechanoradicals generated by the breaking of the first network initiate in situ polymerization of NIPAAm supplied from the internal circulatory flow, and form PNIPAAm chains (red). The thermoresponsive PNIPAAm is detected by fluorescent ANS. Only the broken chain in the DN gel is shown.

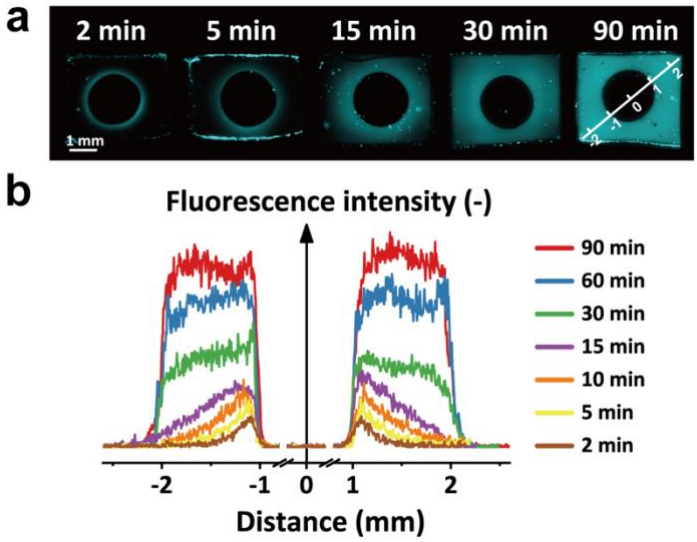


Figure 4.6.Visualization of the diffusion of the monomer molecules by fluorescence distribution. (a) Fluorescent images of the pre-flow cross-sectional slices, the white scale bar arranged in a diagonal direction on the 90 min sample indicates the position to measure the line profiles of fluorescence intensity in 'b'. (b) Fluorescence intensity line profiles of the cross-sectional slices of the preflow samples with various flow times.

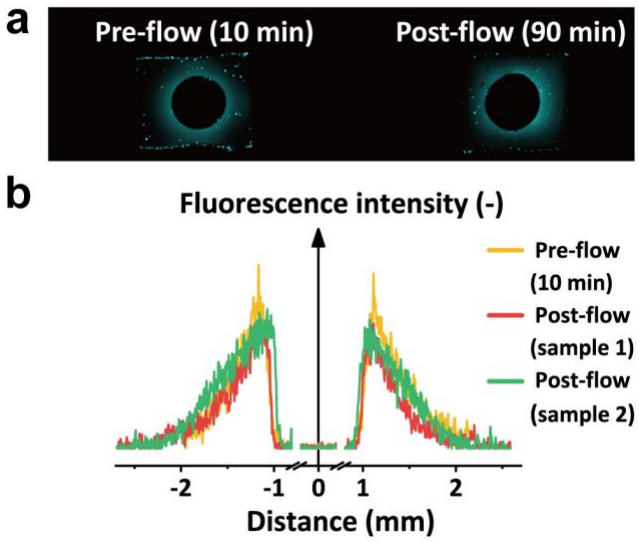


Figure 4.7. (a) Fluorescent images of the cross-sectional slices of the c-DN gels of pre-flow (10 minutes) and post-flow (90 minutes). (b) Fluorescence intensity line profiles of the pre-flow (10 min) and two parallel post-flow samples, by which the mechanoradical lifetime is presumed to be 10 minutes.

4.5. References

1 Z. S. Kean and S. L. Craig, “Mechanochemical remodeling of synthetic polymers”, *Polymer*, 2012, **53**, 1035-1048.

2 T. Ouchi, B. H. Bowser, T. B. Kouznetsova, X. J. Zheng and S. L. Craig, “Strain-triggered acidification in a double-network hydrogel enabled by multi-functional transduction of molecular mechanochemistry”, *Materials Horizons*, 2023, **10**, 585-593.

3 H. T. Baytekin, B. Baytekin and B. A. Grzybowski, “Mechanoradicals Created in "Polymeric Sponges" Drive Reactions in Aqueous Media”, *Angewandte Chemie-International Edition*, 2012, **51**, 3596-3600.

4 B. Rennekamp, C. Karfusehr, M. Kurth, A. Uenal, D. Monego, K. Riedmiller, G. Gryn'ova, D. M. Hudson and F. Graeter, “Collagen breaks at weak sacrificial bonds taming its mechanoradicals”, *Nature Communications*, 2023, **14**, 2075

5 T. Matsuda, R. Kawakami, R. Namba, T. Nakajima and J. P. Gong, “Mechanoresponsive self-growing hydrogels inspired by muscle training”, *Science*, 2019, **363**, 504-508.

6 Y. H. Na, T. Kurokawa, Y. Katsuyama, H. Tsukeshiba, J. P. Gong, Y. Osada, S. Okabe, T. Karino and M. Shibayama, “Structural characteristics of double network gels with extremely high mechanical strength”, *Macromolecules*, 2004, **37**, 5370-5374.

7 Z. J. Wang, J. L. Jiang, Q. F. Mu, S. Maeda, T. Nakajima and J. P. Gong, “Azo-Crosslinked Double-Network Hydrogels Enabling Highly Efficient Mechanoradical Generation”, *Journal of the American Chemical Society*, 2022, **144**, 3154-3161.

8 C. Walling, “Fenton’s Reagent Revisited”, *Accounts of Chemical Research*, 1975, **8**, 125-131.

9 W. H. Koppenol, “The Centennial of the Fenton Reaction”, *Free Radical Biology and Medicine*, 1993, **15**, 645-651.

10 T. Matsuda, R. Kawakami, T. Nakajima and J. P. Gong, “Crack Tip Field of a

Double-Network Gel: Visualization of Covalent Bond Scission through Mechanoradical Polymerization", *Macromolecules*, 2020, **53**, 8787-8795.

11 D. Ito and H. Itagaki, "Clarification of the inner microenvironments in poly(N-isopropylacrylamide) hydrogels in macrogel and microgel forms using a fluorescent probe technique", *European Polymer Journal*, 2018, **99**, 277-283.

12 D. C. Turner and L. Brand, "Quantitative Estimation of Protein Binding Site Polarity . Fluorescence of N-Arylaminonaphthalenesulfonates", *Biochemistry*, 1968, **7**, 3381-3390.

13 M. H. Futscher, M. Philipp, P. Muller-Buschbaum and A. Schulte, "The Role of Backbone Hydration of Poly(N-isopropyl acrylamide) Across the Volume Phase Transition Compared to its Monomer", *Scientific Reports*, 2017, **7**.

14 X. Z. Zhang, X. D. Xu, S. X. Cheng and R. X. Zhuo, "Strategies to improve the response rate of thermosensitive PNIPAAm hydrogels", *Soft Matter*, 2008, **4**, 385-391.

15 S. Zhu, Y. Tian, A. E. Hamielec and D. R. Eaton, "Radical Concentrations in Free-Radical Copolymerization of Mma/Egdma", *Polymer*, 1990, **31**, 154-159.

16 K. S. Anseth and C. N. Bowman, "Kinetic Gelation Predictions of Species Aggregation in Tetrafunctional Monomer Polymerizations", *Journal of Polymer Science Part B-Polymer Physics*, 1995, **33**, 1769-1780.

17 S. Zhu, Y. Tian, A. E. Hamielec and D. R. Eaton, "Radical Trapping and Termination in Free-Radical Polymerization of Mma", *Macromolecules*, 1990, **23**, 1144-1150.

18 S. Nara, S. Shimada, H. Kashiwabara and J. Sohma, "Relation of Decay of Free Radicals in Irradiated Polyethylene to Molecular Motion of Polymer and Configurations of Free Radicals", *Journal of Polymer Science Part a-2-Polymer Physics*, 1968, **6**, 1435-1449.

19 P. J. Butiagin, "The decay of free radicals in polymer media", *Pure and Applied Chemistry*, 1972, **30**, 57–76.

20 S. Shimada, "Esr Studies on Molecular-Motion and Chemical-Reactions in Solid Polymers in Relation to Structure", *Progress in Polymer Science*, 1992,

17, 1045-1106.

21 S. Shimada and Kashiwab.H, "Decay Reactions of Free-Radicals in Irradiated Polyethylene and Diffusion-Controlled Processes", *Polymer Journal*, 1974, **6**, 448-450.

22 S. I. Ohnishi and I. Nitta, "Rate of Formation and Decay of Free Radicals in Gamma-Irradiated Polymethyl Methacrylate by Means of Electron Spin Resonance Absorption Measurements", *Journal of Polymer Science*, 1959, **38**, 451-458.

23 M. Garg, J. E. Aw, X. Zhang, P. J. Centellas, L. M. Dean, E. M. Lloyd, I. D. Robertson, Y. Q. Liu, M. Yourdkhani, J. S. Moore, P. H. Geubelle and N. R. Sottos, "Rapid synchronized fabrication of vascularized thermosets and composites", *Nature Communications*, 2021, **12**, 2836.

24 R. T. M. Jakobs, S. Ma and R. P. Sijbesma, "Mechanocatalytic Polymerization and Cross-Linking in a Polymeric Matrix", *Acs Macro Letters*, 2013, **2**, 613-616.

Chapter 5 Vascular-Like Channel Sustained Self-Growth

5.1. Introduction

Muscle building is a mechanochemical process in which mechanical work is used to trigger chemical reactions for muscle hypertrophy.[1-4] Mechanical training intensity and frequency influence the extent of damage to muscle fibers, while nutrients such as amino acids and minerals chemically affect tissue reconstruction.[5] Muscle growth provides a fascinating model for material innovations. one problem for a better usages of DN gels as the next generation of muscle-mimicking materials is that: a constant supply to complement the monomer consumption during the force-triggered mechanoradical polymerization,[6] thus an opening system filled with monomer solution is required during stretching in order to sustain the mechanoradical polymerization, such an under-solution system largely confines their observations and usages.

In this chapter, inspired by the vascular structures in nature,[7-10] we proposed a mechanochemical strategy for hydrogel growth by using c-DN hydrogels. In previous studies, the DN hydrogels were immersed in monomer solutions during the mechanochemical process to replenish the monomers, which significantly limited their usage. The circulatory system constructed by vascular channel enabled a sustainable supply of monomers to c-DN hydrogels. This self-sustainable system can simultaneously control the circulation of the monomer solutions and mechanical deformation. Using this system, we successfully achieved the continuous muscle-like hypertrophy of DN gels in deoxygenated air. We also used this system to investigate the kinetics of mechanochemical growth in DN gels. With the continuous circulation of the monomers, an extended polymerization time (~1 h) was observed using Raman

spectroscopy. We discuss this unique polymerization behavior from the viewpoint of the possible long lifetimes of mechanoradicals tethered to a polymer network.

5.2. Experiments

5.2.1. Self-Growth of c-DN Gel Supplied by Channel Flow

We used the commercial tensile tester (MCT-2150, A&D Co.) inside a glove box to apply a cyclic tensile force trigger on the hydrogel. The upper jig was moved cyclically following the protocol shown in **Figure 5.1**. The upper jig was moved upward for a displacement of Dp = 105 mm, at which point the gel reached complete necking, and then returned to the neutral position (Dp = 0) of the virgin gel. The crosshead velocity is at 100 mm min^{-1}.

For the cyclic tensile tests performed using a fixed strain, the lower jig was kept stationary (**Figure 5.2**), and the upper jig was moved following the protocol shown in **Figure 5.1.**

For the cyclic tensile tests performed using a fixed tensile force, the lower end of the c-DN gel was connected to a weight. A 0.3 kg weight was used to induce the yielding of the virgin c-DN gel (**Figure 5.3**).

5.2.2. SEM Observation Before and After Self-Growth

To prepare samples for scanning electron microscopy (SEM, JSM-6010LA, JEOL Ltd.), $M_{0.10}C_{0.10}$ and $M_{0.04}C_{0.04}$ gels were collected after the fourth stretch and immersed in a large volume of water to remove unreacted monomers. After reaching a new equilibrium state, the samples were freeze-dried (Advantage XL-70, VirTis freeze-dryer), and the gel surface was coated with gold using an ion-sputtering device (E-1010, Hitachi, Japan).

5.2.3. Raman Spectroscopy for Detecting Constitution Change

Raman spectroscopy (RENISHAW, inVia Reflex) was performed using 532-nm laser as an excitation source, and the incident power was set to 10 mW. The focal spot was adjusted to the channel wall of the c-DN gel. For quantification, a similar area of each sample (middle part of the gauge) was considered for detection. For the c-DN gels subjected to repeated cyclic tensile tests, the $M_{0.10}C_{0.10}$ and $M_{0.04}C_{0.04}$ gels were collected after each stretch.

To detect the progress of mechanochemical growth, $M_{0.10}C_{0.10}$ gels grown for various durations (5–360 min) after the first stretch were collected. To quench the mechanoradical polymerization, the samples were removed from the deoxygenated atmosphere immediately after growth of a preset time. The gels were then immersed in a large volume of distilled water for one week, during which we repeatedly exchanged the soaking water to remove unreacted monomers before the Raman measurements.

5.3. Results and Discussion

5.3.1. Muscle-Like Cyclic Strengthening Sustained by Continuous Flow

To achieve self-strengthening, an elastically effective network needs to be formed in the sample via mechanoradical polymerization. Therefore, an aqueous solution containing NaAMPS as a monomer and N,N'-methylene- bisacrylamide (MBAA) as a crosslinker was circulated during the cyclic tensile test. The samples were coded as M_aC_b, where a and b are the molar concentrations of the monomer (M) and cross-linker (C), respectively, in the flow solution. For example, the $M_{0.10}C_{0.10}$ sample indicates a flow solution containing 0.10 M NaAMPS and 0.10 M MBAA. Before the cyclic tensile test, the sample was circulated for 1.5 h to allow the reactants in the c-DN gel to reach

equilibrium. After each loading–unloading cycle, a resting time of 1 h was set before the next cycle.

First, cyclic tensile tests were performed using a fixed tensile force. Therefore, the lower end of the c-DN gel was connected to a weight. A 0.3 kg weight was used to induce the yielding of the virgin c-DN gel. The upper jig was moved cyclically following the protocol shown in **Figure 5.1**.

Figure 5.4 shows the images of the muscle-like strengthening behavior of $M_{0.10}C_{0.10}$. As indicated by the line marking the locations of the weight attached to the lower jig, although the weight remained still in the first cycle, it was raised to higher locations in successive loadings, resembling muscles that became stronger and lifted weights during strength training. The difference in the weight-lifted height between each cycle gradually decreased, indicating that the c-DN gel became stiffer with the cyclic lifting.

Subsequently, cyclic tensile tests were conducted under a fixed tensile strain. In this test, the lower jig was kept stationary, and the upper jig was moved upward for a displacement of Dp = 105 mm, at which point the gel reached complete necking and then returned to the neutral position (Dp = 0) of the virgin gel (**Figure 5.1**). As a typical example, the force profile of the $M_{0.10}C_{0.10}$ sample in response to cyclic tensile deformation is shown in **Figure 5.5**. The response of the $M_{0.00}C_{0.00}$ sample (perfused with pure water) is shown for comparison. The $M_{0.10}C_{0.10}$ sample showed successive strengthening with cyclic loading, as evidenced by the force curve surpassing the previous curve, whereas the $M_{0.00}C_{0.00}$ sample (perfused with pure water) showed no strengthening.

5.3.2. Tunable Self-Growth in Response to Channel Flow

The strengthening effect in the solution strongly depended on the concentrations of the monomer and cross-linker in the solution. The M_aC_b samples can be classified into three groups: no growth, slight growth, and remarkable growth, depending on the flowing monomer and crosslinker concentrations (**Figure 5.6**).

Sample $M_{0.08}C_{0.0}$ with no crosslinker exhibited no strengthening, similar to $M_{0.00}C_{0.00}$, confirming that the newly formed polymer must be crosslinked for strengthening. Samples of $M_{0.02}C_{0.02}$ and $M_{0.00}C_{0.04}$ showed slight growth, indicating that only a sparse network was formed at low monomer and crosslinker concentrations, the original tensile force-displacement curves shown in **Figure 5.7 and 5.8**.

There is a positive correlation between the mechanical enhancement and the supply concentration, simply exhibit an "the more the better" effect. Samples of $a = b \geq 0.04$ M showed remarkable growth and successive strengthening was observed with the cyclic tensile loading. The increasing trend may explain the rationale of the repeated self-strengthening: that the mechanoradical polymerization supplied by enough amount of monomer and cross-linker (above 0.04 M) would build the matrix network to a denser state, the newly formed network also prepare for sacrificing itself to originate chain-end radicals, thus initiate polymerization in the next cycle.

5.3.3. Volume Growth

As shown in **Figure 5.7**, The critical displacement to show the force gradually increased with the number of cycles owing to an increase in the gauge length by growth, whereas that of the $M_{0.00}C_{0.00}$ sample hardly changed. What is more, combined with the cross-sectional size of self-grown samples (**Figure 5.9**), we can draw the conclusion that the strength and size of the samples both increased by remodeling the structure under cyclic

mechanical training. We observed four translucent “scars” outside the gauge region, which distinctly indicate the occurrence of four times of self-strengthening (**Figure 5.10**). As the gauge region yielded by stretching, it became stiffer owing to self-strengthening. Therefore, the relatively “weaker part” outside the yielded part started to yield in the next stretch cycle to show the training scars.

5.3.4. Quantification of Mechanical Self-Growth

To quantify the extent of self-growth, the yield force (F_y), stiffness, and hysteresis were measured, as shown in **Figure 5.11**. The parameters summarized from the force–displacement curves are compared in **Figure 5.12**. For the $M_{0.10}C_{0.10}$, $M_{0.08}C_{0.08}$, and $M_{0.04}C_{0.04}$ samples, F_y, stiffness, and hysteresis all showed increasing trends from the second to the fourth cycle.

Because a higher yield force and stiffness correspond to a denser network, the increasing trend indicates that a denser network was newly formed after each cycle. The hysteresis loop area, which indicates the energy dissipated in the polymer network fracturing at each cycle, increases with the number of cycles. These results indicate that successive structural reconstruction occurs at the expense of the deconstruction of the network formed in the previous cycle. The decrease in stiffness after the first loading, especially for the M_aC_b samples with $a = b < 0.08$ is owing to the partial fracture of highly pre-stretched strands of the initial first network by fracture. The strands in the newly formed network are in a relaxed state and should exhibit lower stiffness than the pre-stretched strands.[11, 12] Nevertheless, the F_y, stiffness, and hysteresis increased with the number of tensile cycles and surpassed those in the first cycle. This indicates that the newly formed network is denser than the first network in the virgin sample.

5.3.5. Quantification of Mechanochemical Growth

The newly formed polymer network increases the polymer density of the c-DN gel. We observed an increase in the polymer mass of the c-DN gel during self-growth. **Figure 5.13** shows scanning electron microscopy (SEM) images of the freeze-dried $M_{0.10}C_{0.10}$ sample before and after four cycles, as described in the previous section. Notably, while the virgin sample exhibited a typical honeycomb-like morphology owing to the evaporation of water, the porous appearance was hardly observed after four training cycles. The latter indicates an increase in the polymer content by mechanoradical polymerization.

The increase in polymer content was then quantitatively analyzed using Raman spectroscopy, which allowed the study of the changes in the chemical composition of the hydrogel. Here, we collected the Raman spectra of the $M_{0.10}C_{0.10}$ (**Figure 5.14**) and $M_{0.04}C_{0.04}$ (**Figure 5.15**) samples in their new equilibrium state after self-growth, and Gaussian fitting was used to analyze the relative content changes caused by the mechanochemical growth. Assignments to Raman bands were summarized in **Table 5.1.**

The band intensity at 1045 cm^{-1}, corresponding to the S=O stretching of NaAMPS units,[13] increased gradually with more tensile cycles, which is a direct chemical proof of the newly formed PNaAMPS network by the mechanochemical process.[14] The peak at 1630 cm^{-1}, corresponding to the NH_2 scissoring vibrations of the PAAm second network,[15, 16] remained constant during mechanoradical polymerization , as expected. By measuring the ratio R of the absolute areas of the peaks at 1045 cm^{-1} (marked in blue) and 1630 cm^{-1} (marked in red), we estimated the molar ratio *f* of the NaAMPS units relative to AAm units in the c-DN gel using the following equation:

$$f_i = f_0(R_i/R_0), \quad (1)$$

where f_i and f_0 are the molar ratios of NaAMPS units to AAm units in the i^{th} and 0^{th} (virgin c-DN gel) cycles, respectively, and R_i and R_0 are the area ratios of the peak at 1045 cm^{-1} to that at 1630 cm^{-1} in the i^{th} and 0^{th} cycles, respectively. The initial molar ratio f_0 (0.015) was calculated from the reagents added during c-DN gel fabrication, neglecting the small-quantity components of the crosslinker and initiator. **Figure 5.16** shows the molar ratio f as a function of the mechanical training cycles for the $M_{0.04}C_{0.04}$ and $M_{0.10}C_{0.10}$ samples. Although the $M_{0.04}C_{0.04}$ sample showed a remarkable decrease in stiffness after the first cycle, as shown in **Figure 5.12**, polymer growth was clearly observed after the first cycle and increased with cyclic mechanical training. Moreover, the amount of polymer growth in $M_{0.10}C_{0.10}$ was larger than that in $M_{0.04}C_{0.04}$. This is consistent with the more efficient mechanical training of the $M_{0.10}C_{0.10}$ sample observed **Figure 5.12**.

5.3.6. Delayed Strengthening after Polymer Growth

Similar to the strengthening and hypertrophy of muscles, the self-growth of DN gels requires time for mechanochemical reactions. In this study, the kinetics of mechanochemical growth and strengthening were investigated. As shown by the protocol in **Figure 5.17**, we applied the first stretch cycle to trigger mechanoradical generation in the gels and then allowed the gels to rest for a preset time varying from 5 to 360 min to allow new network formation in the gels. Subsequently, we applied a second stretch cycle to measure the mechanical enhancement of the gels by growth during the rest time. During the entire process, the c-DN gels were continuously circulated with the aqueous solution containing 0.1 M NaAMPS monomer and 0.1 M MBAA crosslinker ($M_{0.10}C_{0.10}$).

Figure 5.18 shows the force–displacement curves of the first and second

stretching cycles. The stiffness and hysteresis as a function of the resting time were extracted from the curves of the second cycle, as shown in **Figure 5.19**. These results clearly show that the gels achieved remarkable strengthening in ~1 h, and then gradually reached a constant state, although the monomers were continuously supplied to the gels by circulation throughout the entire process.

The growth of the PNaAMPS at different resting times was further detected by Raman spectroscopy, and the results are shown in **Figure 5.20**. The peak signal from PNaAMPS at 1045 cm^{-1} increased with resting time up to 360 min. The molar ratios *f* of NaAMPS units relative to the AAm units at various time was calculated from the corresponding area ratio of the peak at 1045 cm^{-1} to that at 1630 cm^{-1}, as shown in **Figure 5.21**. We observed that PNaAMPS had more than double its original molar ratio within 5 min, more than half of the total newly formed PNaAMPS for a growth time of 360 min.

Compared with **Figure 5.20**, we noticed that the hysteresis and stiffness only exhibited a mild increase in the first 5 min. This delayed strengthening compared to polymer growth is further highlighted in the plots of stiffness and hysteresis as a function of the molar ratio *f* in **Figure 5.22**. The results show that the newly formed PNaAMPS can only strengthen the gels above a critical content ($f = 0.03$), which is twice that of the virgin DN gels ($f = 0.015$). Such a discrepancy in the kinetics of polymer growth and mechanical strengthening can be attributed to the delayed cross-linking reaction compared to monomer polymerization . To form a network structure, both functional groups of the MBAA crosslinker should be incorporated into the network.[17] Once one functional group is incorporated into the polymer, the other has a lower probability of being incorporated owing to the low mobility of the polymers tethered to the existing network.

Surprisingly, mechanoradical polymerization in the c-DN gels lasted for hours with a continuous monomer supply from the circulating channel. Because polymerization was triggered by the mechanoradicals generated in the first stretch cycle at a concentration of ～10 mM, the observed growth of PNaAMPS indicates that some radicals were still alive at 360 min. We conjecture that the growing polymers that are tethered to the network have a very low probability of chain termination reactions owing to suppressed thermal motion, such as the grafting of radicals and a crowding environment. Such long-existing macro- radicals are more commonly discussed in glassy or crystalline polymers such as polyethylene and polymethylmethacrylate.[17-21] This unique feature of mechanoradical reactions in DN gels needs to be studied in detail in future work.

5.4. Conclusions

Here, in order to attain continuous growth in response to repetitive mechanical stimuli with a constant supply, we incorporated a vascular channel inside the DN hydrogel as a delivering pathway, whereby attaining a continuous polymer growth in response to repetitive mechanical stimuli with an independent and constant monomer complementation. Mechanoradical polymerizations in the presence of a sufficient amount of monomer and crosslinker ($a = b \geq 0.04$ M) resulted in an elastically effective new network. The newly formed densely crosslinked network not only enhanced the mechanical performance of the c-DN hydrogel but also sacrificed itself to generate mechanoradicals upon force triggers. We also noticed the necessity of both monomers and cross-linkers for the co-building process of the new network, it also need enough amount of the chemical building blocks to form elastically effective crosslinked load-bearing chains that impart additional mechanical enhancement to the sample.

Remodeling and growth of c-DN gels in response to repeated mechanical stimuli is therefore achieved by a vascular-like replenishing of the monomers consumed during polymerization. Building upon the structural foundation provided by the c-DN gel, we were able to make a step further into the observation of both mechanical and chemical growth trends in the process of the mechanoradical polymerization in DN hydrogels.

Figures

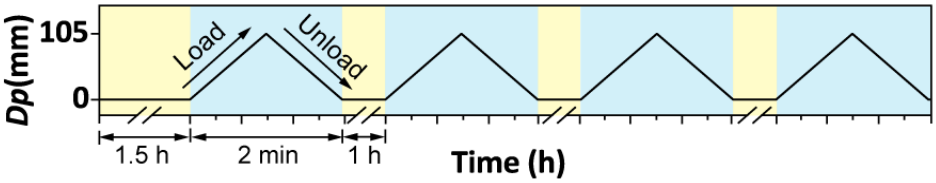


Figure 5.1. Protocol of the upper crosshead displacement during the cyclic deformation of the c-DN gel (gauge length = 15 mm).

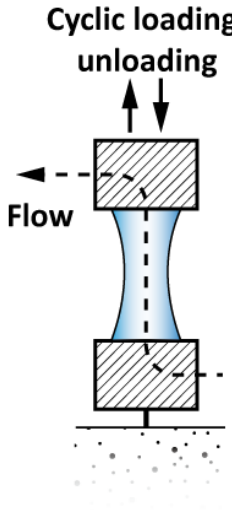


Figure 5.2. Illustrator of the setup for cyclic tensile tests.

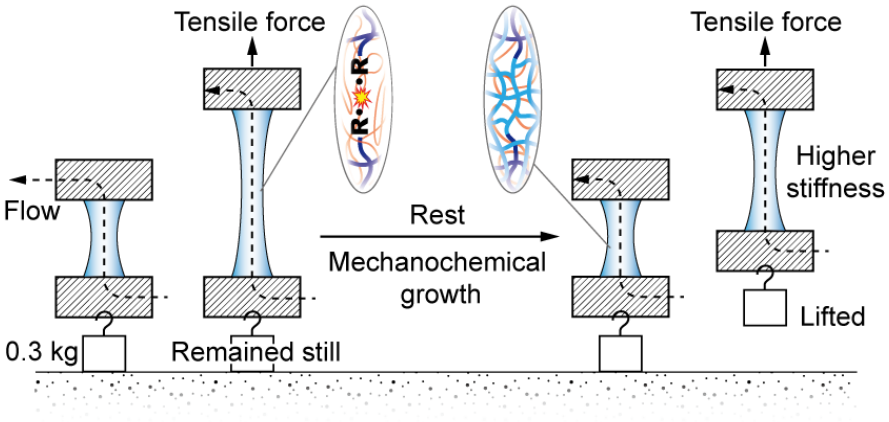


Figure 5.3. Illustration of the training process of the c-DN hydrogel by mechanochemical growth. The upper jig is fixed to the tensile tester and repeatedly lifted up to a displacement of 105 mm, the lower jig is connected to a weight (0.3 kg). After the ‘‘training’’ sustained independently by the vascular perfusion, the c-DN hydrogel is able to lift up the weight.

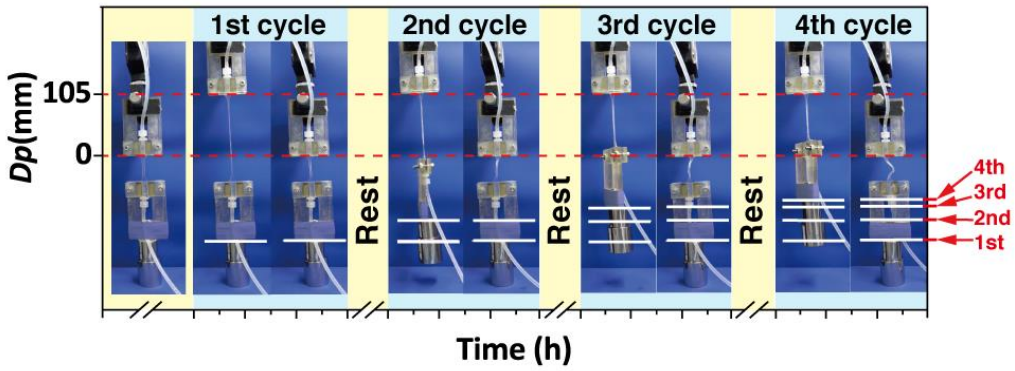


Figure 5.4. Demonstrations of the muscle-like behaviours of a c-DN hydrogel supplied by 0.10 M NaAMPS monomer and 0.10 M MBAA crosslinker ($M_{0.10}C_{0.10}$) showing repetitive stretch-triggered mechanical growth

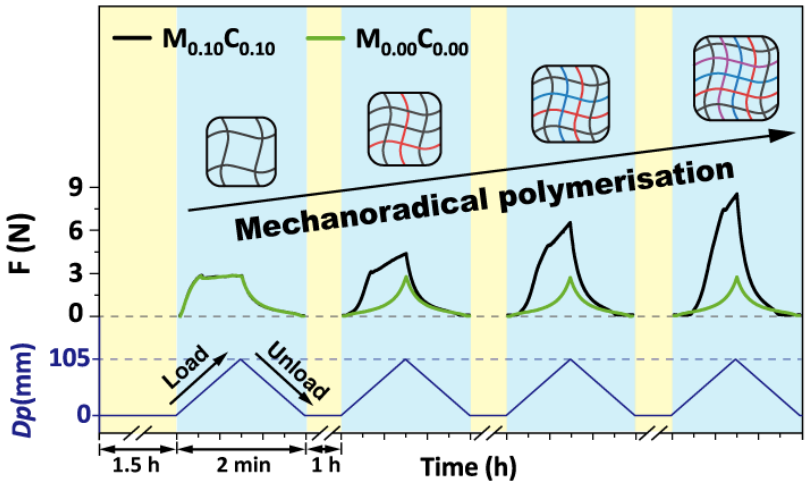


Figure 5.5. Force–time curves of $M_{0.10}C_{0.10}$ under a repeated tensile force trigger shown in the loading–unloading protocol underneath: the upper crosshead displacement (*Dp*) is lifted up to 105 mm and then returned to the original position (*Dp* = 0 mm) during the cyclic deformation of the c-DN gel (gauge length = 15 mm). The gel shows an noticeable strengthening due to repeated network deconstruction–reconstruction. $M_{0.00}C_{0.00}$ implies the flow of pure water as a reference, which indicates no self-growth without monomers supply from the channel. Samples are coded by the concentrations of monomer and cross-linker in the flowing solution as M_aC_b, where "a" stands for the monomer (NaAMPS) concentration and "b" the cross-linker (MBAA) concentration (all in mol/L).

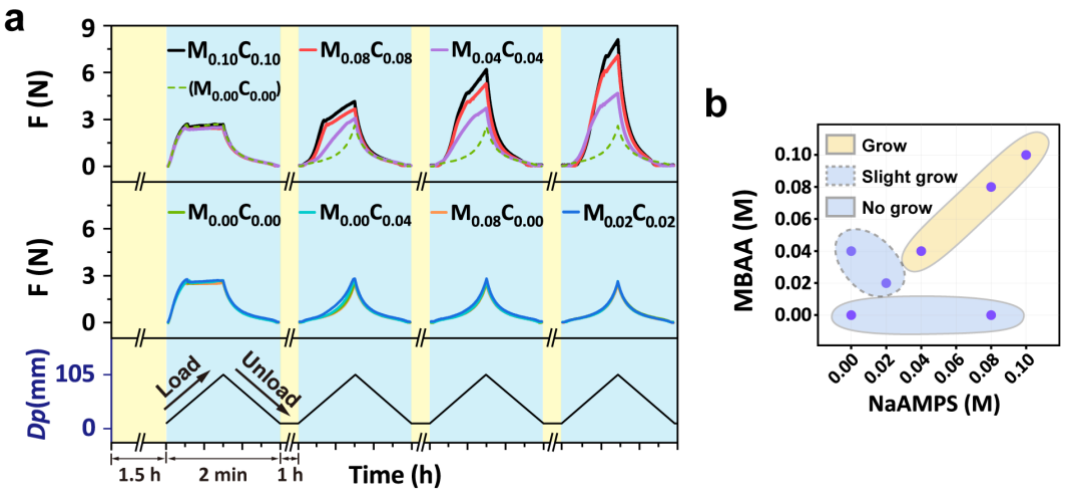


Figure 5.6. Effect of monomer and cross-linker concentration supplied through the channel on self-strengthening. (a) Result of force enhancement of various samples as a function of time, the loading–unloading process is conducted as the protocol in the lower panel, groups shown in the upper panel ($M_{0.10}C_{0.10}$, $M_{0.08}C_{0.08}$, $M_{0.04}C_{0.04}$) exhibit noticeable self-growth ($M_{0.00}C_{0.00}$ implies the flow of pure water as a blank control group), while the middle panel ($M_{0.00}C_{0.00}$, $M_{0.00}C_{0.04}$, $M_{0.08}C_{0.00}$, $M_{0.02}C_{0.02}$) exhibits only slight or no self-growth. (b) Group summary according to the reactant supply and self-growth result.

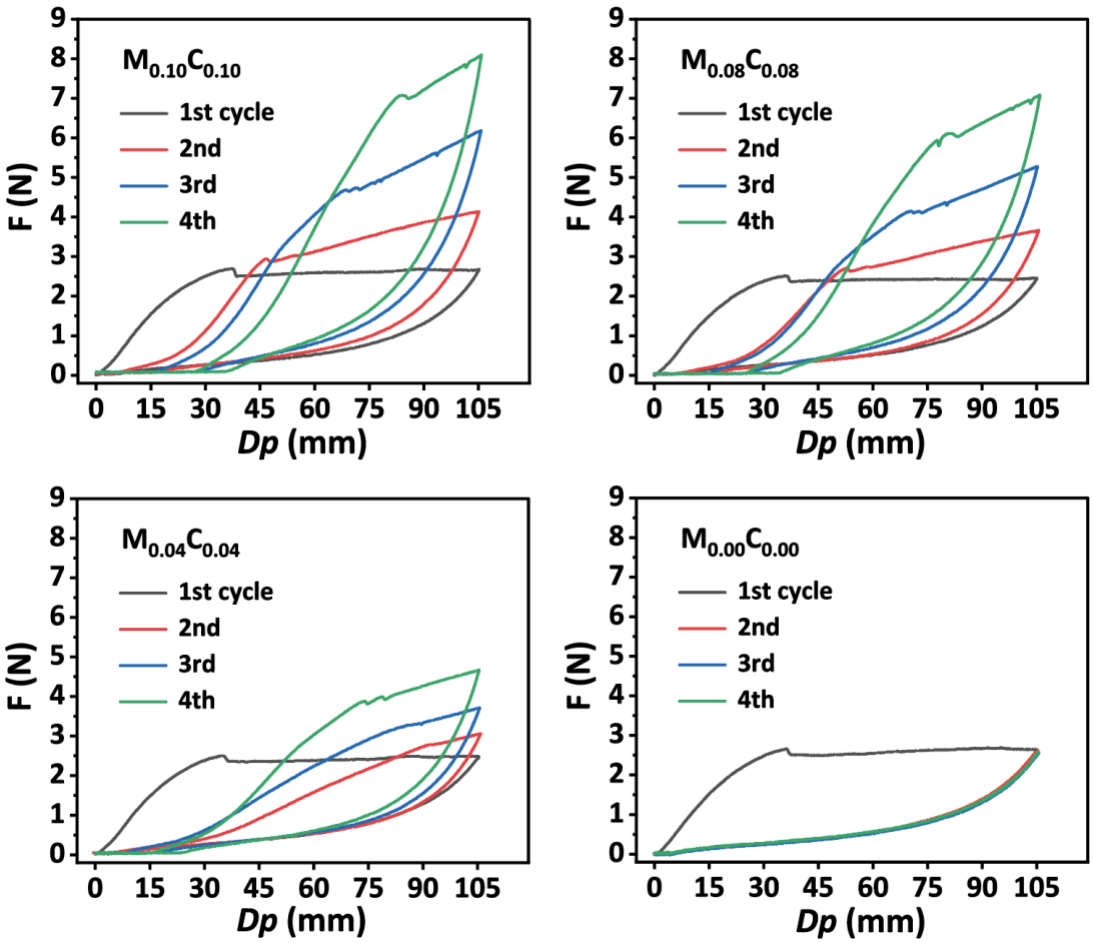


Figure 5.7. Force–displacement curves of the four times of cyclic loading–unloading under supply of monomers and cross-likers of various concentrations. The results are replotted to the force–time curves in Figure 5.6 (upper panel).

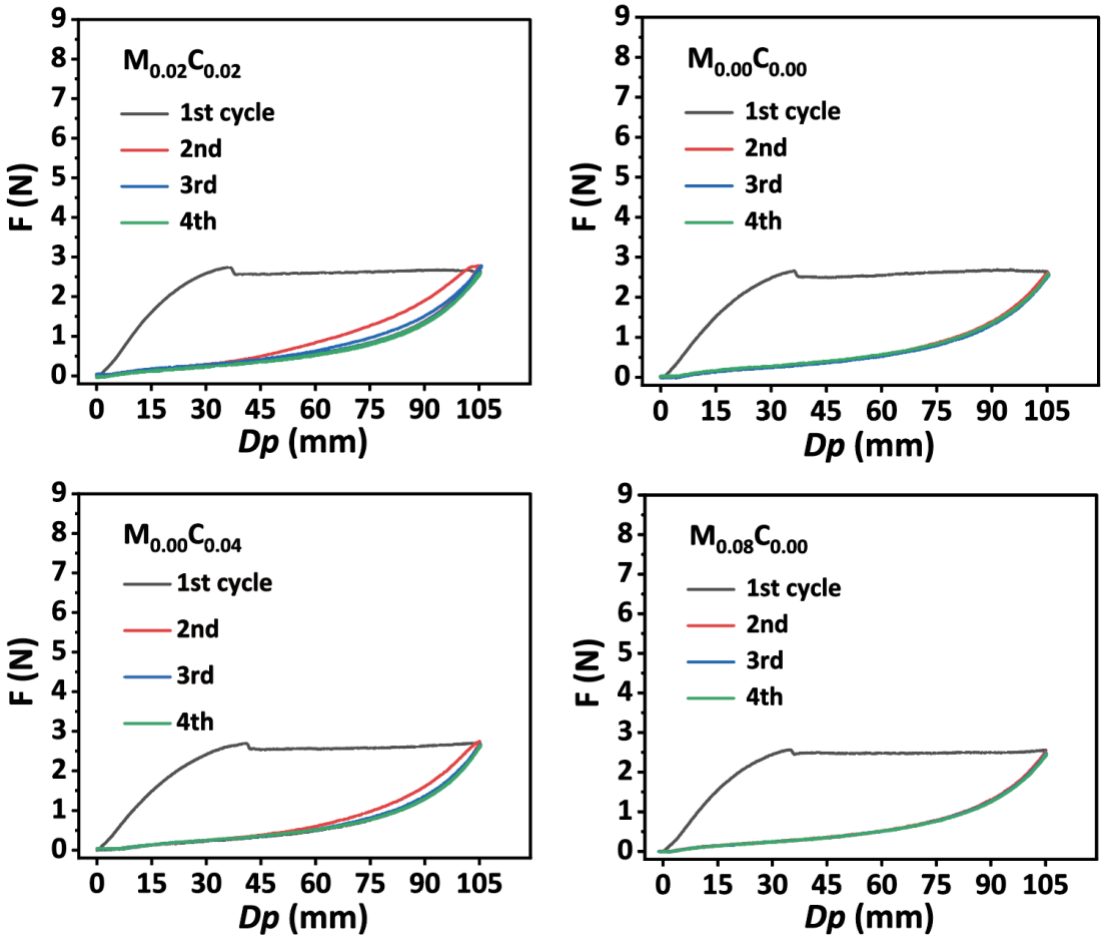


Figure 5.8. Force–displacement curves of the four times of cyclic loading–unloading under supply of monomers and cross-likers of various concentrations. The results are replotted to the force–time curves in Figure 5.6 (middle panel).

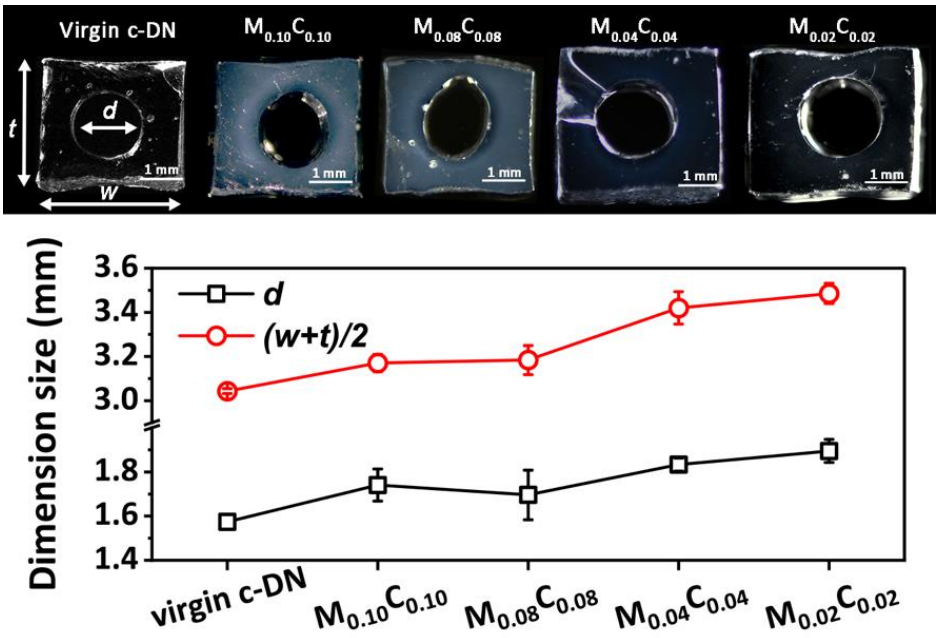


Figure 5.9. Photographs of the c-DN gel slices supplied with various monomer and crosslinker concentrations and their corresponding cross-sectional size after one tensile cycle, the $M_{0.10}C_{0.10}$ and $M_{0.08}C_{0.08}$ exhibit little swelling owing to the densely cross-linked network.

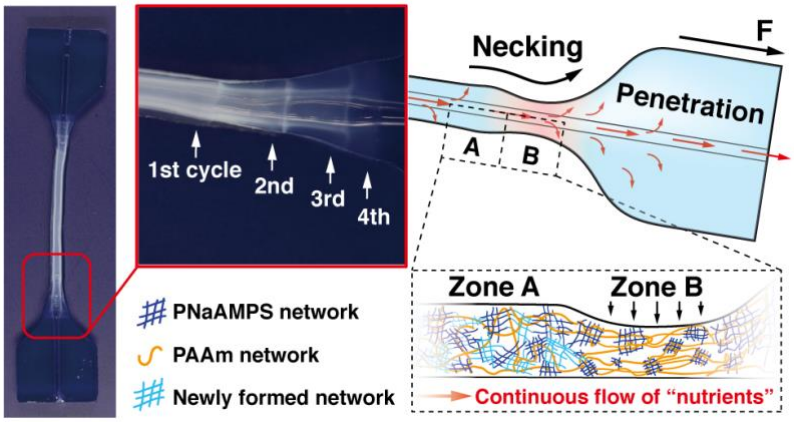


Figure 5.10. Appearance of $M_{0.10}C_{0.10}$ sample after four times of self-growth and the illustration of the unevenly distributed structure which caused the whitening phenomenon. As the gauge region yielded by stretch, it became stiffer by self-strengthening. Therefore, the relatively "weaker part" outside the yielded zone starts to yield in the next stretch. Thus, translucent "scars" of "training" that distinctly indicates the occurrence of four times of self-strengthening were left.

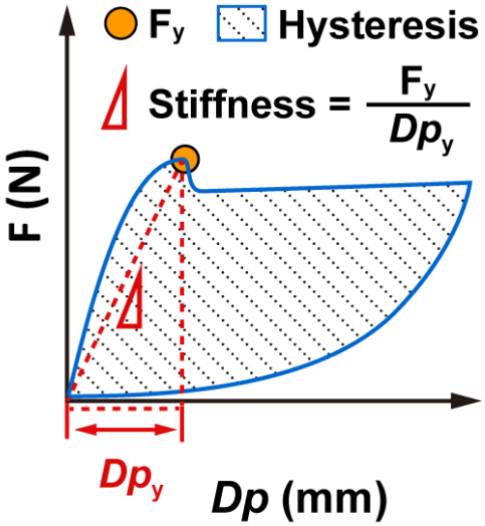


Figure 5.11. Definition of mechanical parameters for evaluating the extent of self-growth from the loading–unloading curve of a cyclic tensile test.

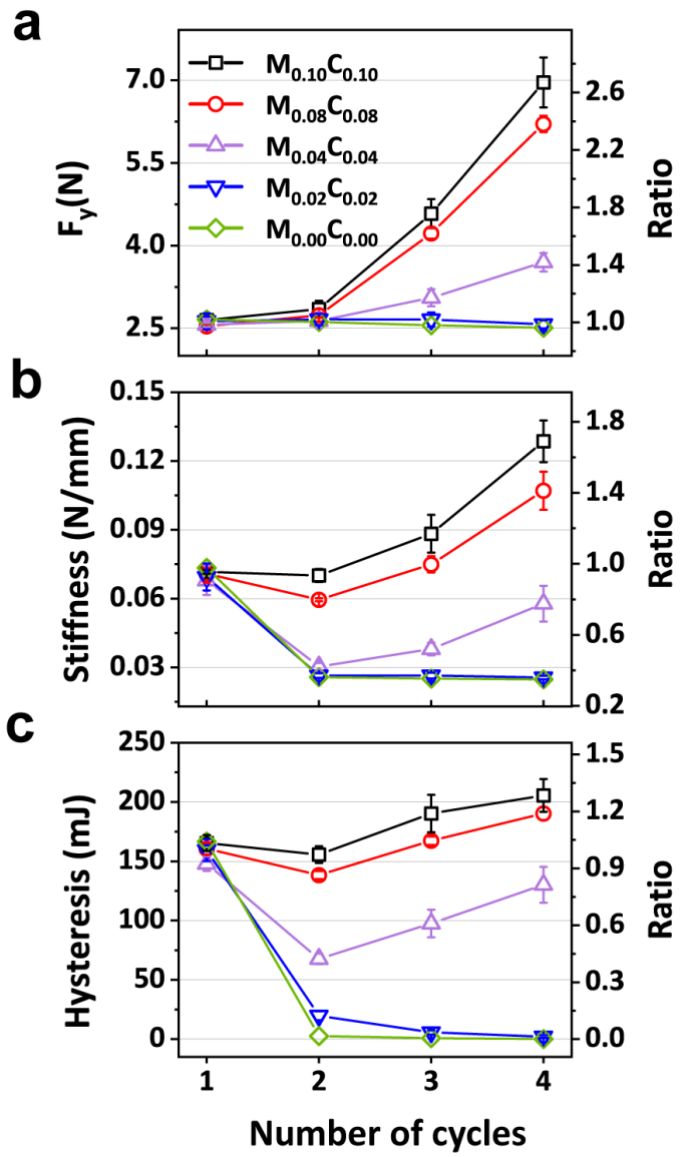


Figure 5.12. Variations and the ratio of change that are relative to the original value of mechanical parameters during four times of self-growth: a. yield force (F_y); b. stiffness; and c. hysteresis

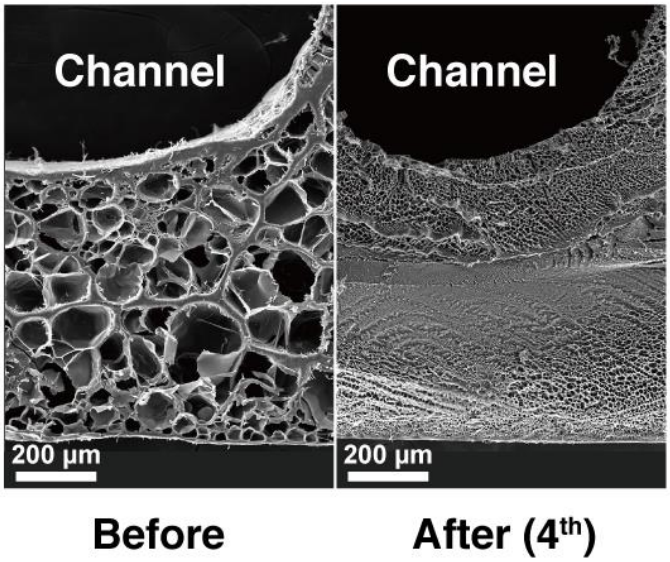


Figure 5.13. Cross-sectional SEM images of the c-DN gel ($M_{0.10}C_{0.10}$) before, and after the fourth cycle of tensile force-triggered mechanoradical polymerization (scale bar: 200 µm).

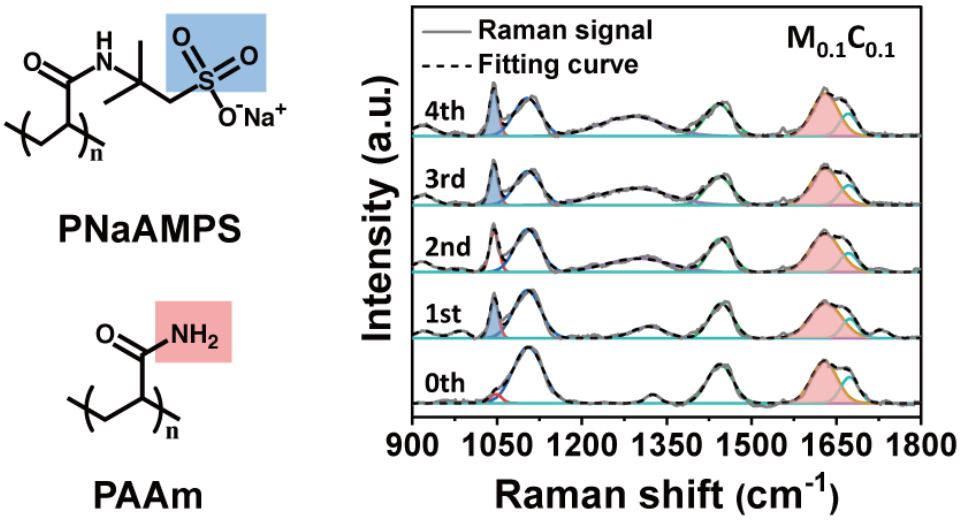


Figure 5.14. Raman spectroscopy of $M_{0.10}C_{0.10}$ samples during four times of stretch, the fitted peak at 1045 cm^{-1} corresponds to the S=O stretching in PNaAMPS (marked as blue), and the peak at 1630 cm^{-1} corresponds to the NH_2 scissoring in PAAm (marked as red).

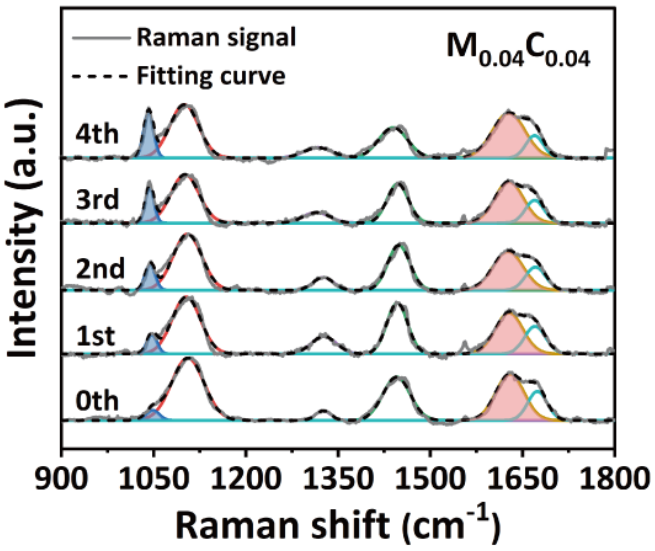


Figure 5.15. Raman spectroscopy of c-DN samples during four times stretching with simultaneous supply of the solution containing 0.04 M NaAMPS monomer and 0.04 M MBAA cross-linker. The peak at 1045 cm^{-1} corresponds to the S=O stretching in PNaAMPS (marked as blue), and the peak at 1630 cm^{-1} corresponds to the NH_2 scissoring in PAAm (marked as red).

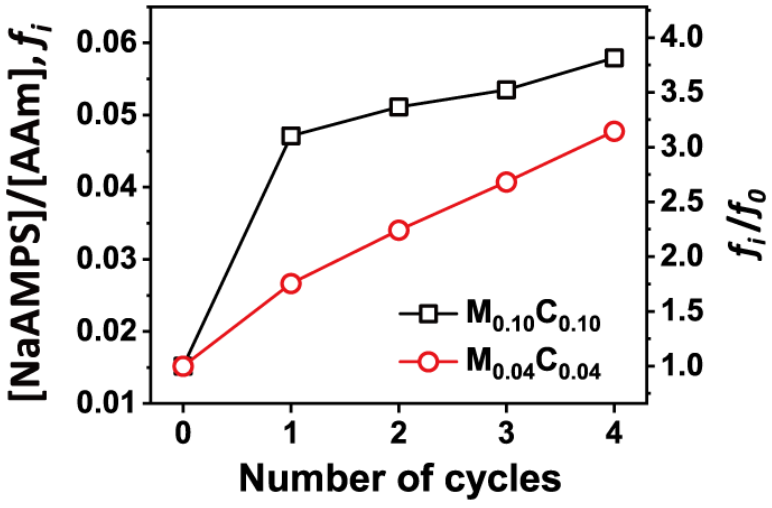


Figure 5.16. Molar ratio of the NaAMPS units to AAm units in the hydrogel matrix as a function of the number of cycles.

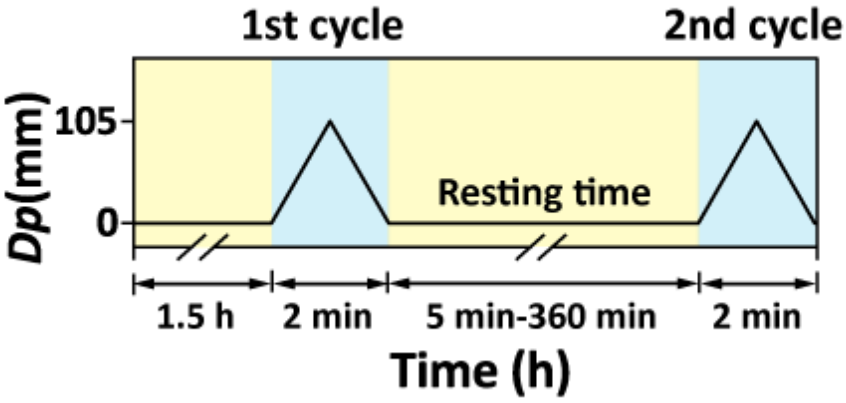


Figure 5.17. Protocol of the two cyclic stretch cycles. A resting time for growth was set between the first and the second cycles. During the whole process, the c-DN gels were continuously circulated with the monomer solution (0.1 M NaAMPS, 0.1 M MBAA).

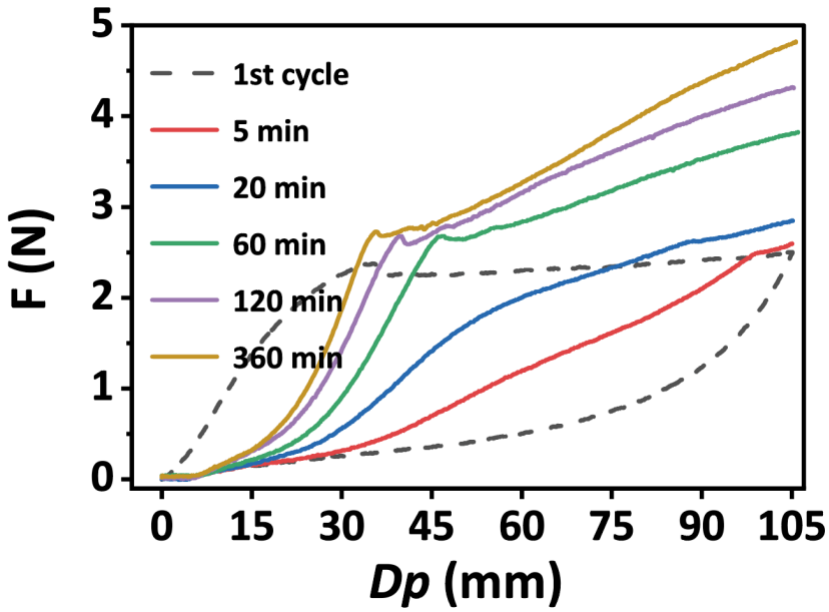


Figure 5.18. Force–displacement curve of the c-DN gels for the first cycle and loading curves of the second cycle after various resting time.

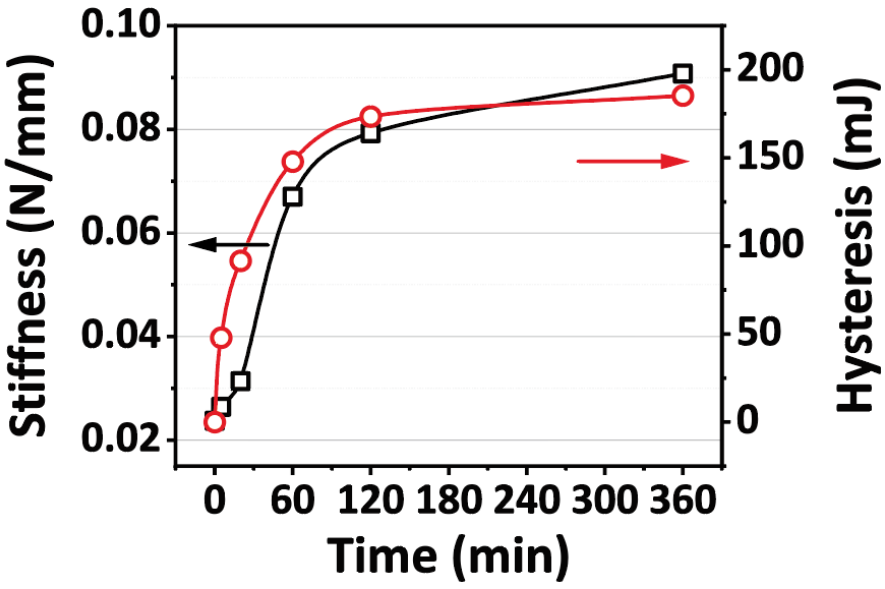


Figure 5.19. Growth-time dependencies of mechanical parameters: stiffness (left axis) and hysteresis (right axis).

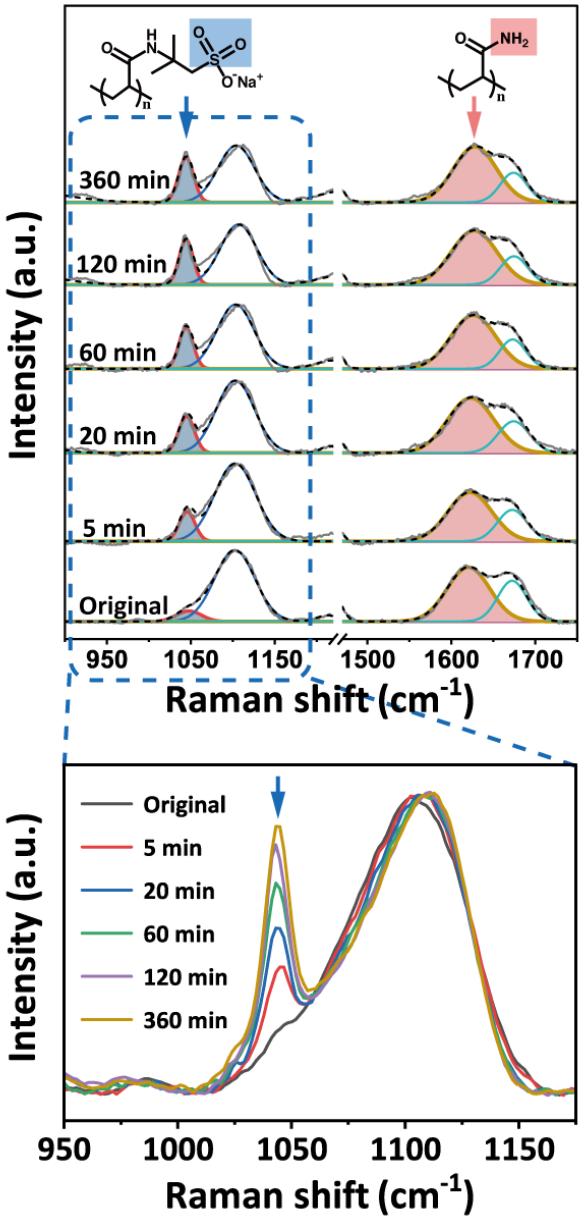


Figure 5.20. Raman spectroscopy and the fitting curves of the $M_{0.10}C_{0.10}$ samples after the second stretch, the Raman signals of the original gel as a reference, the peaks correspond to PNaAMPS and PAAm is marked as blue and red, respectively. The peak at 1045 cm^{-1} pointed by a blue arrow corresponds to the signal of *v* (S=O) originated from the growing PNaAMPS during the resting time.

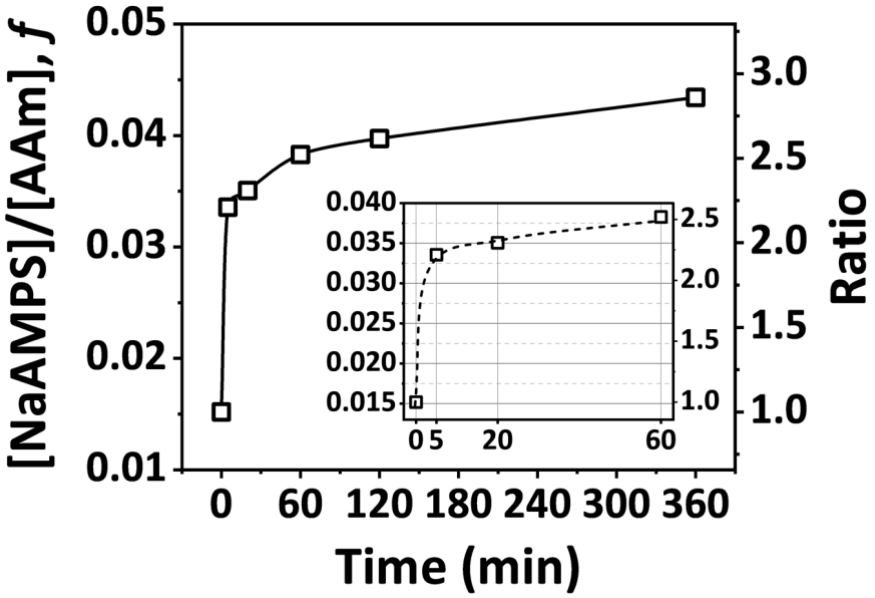


Figure 5.21. Growth-time dependencies of chemical parameters: Unit mole ratio of NaAMPS to AAm (*f*), the inserted figure shows the detailed trend of chemical signals in 60min.

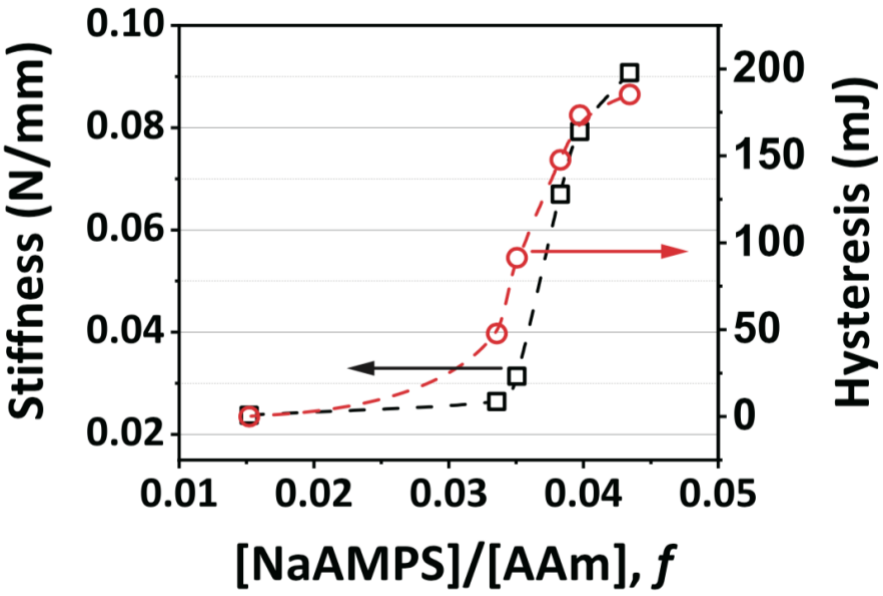


Figure 5.22. Correlations between the molar ratio of NaAMPS/AAm and stiffness (left axis) and hysteresis (right axis). The dashed line is a visual guide.

Table 5.1 Raman band positions and assignments.

Wavenumber (cm^{-1})	Assignments
1045	S=O stretching[13]
1112	C-C skeletal stretching[22]
1327	CH, NH bending[15, 23]
1457	CH_2 bending[23, 24], CH_3 scissoring[15]
1630	NH_2 scissoring[16, 25-27]
1657	C=O stretching[16, 27]

5.5. References

1 G. J. Laurent, M. P. Sparrow, P. C. Bates and D. J. Millward, “Turnover of Muscle Protein in Fowl - Collagen Content and Turnover in Cardiac and Skeletal-Muscles of Adult Fowl and Changes during Stretch-Induced Growth”, *Biochemical Journal*, 1978, **176**, 419-427.

2 C. W. Kang, M. L. Sunde and R. W. Swick, “Growth and Protein-Turnover in the Skeletal-Muscles of Broiler Chicks”, *Poultry Science*, 1985, **64**, 370-379.

3 D. M. Skjaerlund, D. R. Mulvaney, W. G. Bergen and R. A. Merkel, “Skeletal-Muscle Growth and Protein-Turnover in Neonatal Boars and Barrows”, *Journal of Animal Science*, 1994, **72**, 315-321.

4 K. M. Tarpenning, R. A. Wiswell, S. A. Hawkins and T. J. Marcell, “Influence of weight training exercise and modification of hormonal response on skeletal muscle growth”, *Journal of Science and Medicine in Sport*, 2001, **4**, 431-446.

5 P. S. Hwang and D. S. Willoughby, “Mechanisms Behind Blood Flow-Restricted Training and Its Effect toward Muscle Growth”, *Journal of Strength and Conditioning Research*, 2019, **33**, S167-S179.

6 T. Matsuda, R. Kawakami, R. Namba, T. Nakajima and J. P. Gong, “Mechanoresponsive self-growing hydrogels inspired by muscle training”, *Science*, 2019, **363**, 504-508.

7 J. H. Jung and C. M. Park, “Vascular development in plants: Specification of xylem and phloem tissues”, *Journal of Plant Biology*, 2007, **50**, 301-305.

8 V. S. H. Rao and T. S. L. Radhika, “The Dynamics of the Flow of Blood in the Human Circulatory System”, *Differential Equations and Dynamical Systems*, 2023, **31**, 673-685.

9 Y. M. Cheng, X. L. Liu, X. T. Ma, R. Garcia, K. Belfield and J. Haorah, “Alcohol promotes waste clearance in the CNS via brain vascular reactivity”, *Free Radical Biology and Medicine*, 2019, **143**, 115-126.

10 H. M. Wei, H. M. Jiang, Y. F. Zhou, X. C. Xiao, C. Zhou and X. M. Ji, “Vascular endothelial cells: a fundamental approach for brain waste clearance”, *Brain*,

2023, **146**, 1299-1315.

11 T. Matsuda, T. Nakajima, Y. Fukuda, W. Hong, T. Sakai, T. Kurokawa, U. Chung and J. P. Gong, "Yielding Criteria of Double Network Hydrogels", *Macromolecules*, 2016, **49**, 1865-1872.

12 T. Nakajima, Y. Ozaki, R. Namba, K. Ota, Y. Maida, T. Matsuda, T. Kurokawa and J. P. Gong, "Tough Double-Network Gels and Elastomers from the Nonprestretched First Network", *Acs Macro Letters*, 2019, **8**, 1407-1412.

13 A. Selvarajan, "Raman spectrum of dimethyl sulfoxide (DMSO) and the influence of solvents", *Proceedings of the Indian Academy of Sciences - Section A*, 1966, **64**, 44–50.

14 G. F. Widhopf and S. Lederman, "Specie Concentration Measurements Utilizing Raman Scattering of a Laser Beam", *Aiaa Journal*, 1971, **9**, 309-316.

15 P. Bour, J. Kapitan and V. Baumruk, "Simulation of the Raman optical activity of L-alanyl-L-alanine", *Journal of Physical Chemistry A*, 2001, **105**, 6362-6368.

16 F. D'Amico, B. Rossi, G. Camisasca, F. Bencivenga, A. Gessini, E. Principi, R. Cucini and C. Masciovecchio, "Slow-to-fast transition of hydrogen bond dynamics in acetamide hydration shell formation", *Physical Chemistry Chemical Physics*, 2015, **17**, 10987-10992.

17 S. Abrol, M. J. Caulfield, G. G. Qiao and D. H. Solomon, "Studies on microgels. 5. Synthesis of microgels via living free radical polymerisation", *Polymer*, 2001, **42**, 5987-5991.

18 Z. S. Kean and S. L. Craig, "Mechanochemical remodeling of synthetic polymers", *Polymer*, 2012, **53**, 1035-1048.

19 T. Ouchi, B. H. Bowser, T. B. Kouznetsova, X. J. Zheng and S. L. Craig, "Strain-triggered acidification in a double-network hydrogel enabled by multi-functional transduction of molecular mechanochemistry", *Materials Horizons*, 2023, **10**, 585-593.

20 S. Nara, S. Shimada, H. Kashiwabara and J. Sohma, "Relation of Decay of Free Radicals in Irradiated Polyethylene to Molecular Motion of Polymer and Configurations of Free Radicals", *Journal of Polymer Science Part a-2-*

Polymer Physics, 1968, **6**, 1435-1449.

21 P. J. Butiagin, "The decay of free radicals in polymer media", *Pure and Applied Chemistry*, 1972, **30**, 57–76.

22 M. K. Gupta and R. Bansil, "Laser Raman-Spectroscopy of Polyacrylamide", *Journal of Polymer Science Part B-Polymer Physics*, 1981, **19**, 353-360.

23 J. S. Suh and K. H. Michaelian, "Surface-Enhanced Raman-Spectroscopy of Acrylamide and Polyacrylamide Adsorbed on Silver Colloid Surfaces - Polymerization of Acrylamide on Silver", *Journal of Raman Spectroscopy*, 1987, **18**, 409-414.

24 A. I. Jirasek, C. Duzenli, C. Audet and J. Eldridge, "Characterization of monomer/crosslinker consumption and polymer formation observed in FT-Raman spectra of irradiated polyacrylamide gels", *Physics in Medicine and Biology*, 2001, **46**, 151-165.

25 P. L. Anto, R. J. Anto, H. T. Varghese, C. Y. Panicker, D. Philip and A. G. Brolo, "FT-IR, FT-Raman and SERS spectra of anilinium sulfate", *Journal of Raman Spectroscopy*, 2009, **40**, 1810-1815.

26 M. Reichenbächer and J. r. Popp, *Challenges in molecular structure determination*, Springer, Heidelberg ; New York, 2012.

27 P. G. Puranik and K. V. Ramiah, "Infra-Red Aud Raman Spectroscopic Studies of Amides", *Proceedings of the Indian Academy of Sciences Section A*, 1961, **A 54**, 69-79.

Chapter 6 General Conclusion and Outlook

In this work, we made a step further to study the metabolic-like growth system that enabled a long-term mechanochemical growth of double-network (DN) hydrogels in air. Based on the foundation that DN hydrogels can generate a high concentration of mechanoradicals owing to the sacrificial bond cleavage when subjected to mechanical deformations. When monitoring the component change of DN gel during self-growth, issues come from the replenish method of monomers, the supply of mechanoradical polymerization sustained by the open system filled with monomer solution may not suitable for practical uses, and difficult to observe the gel during growing.

Therefore here we intend to construct a channel structure for the vascular-like monomer supply. To continuously deliver monomers for the mechanoradical polymerization in DN gels, a channel-containing double-network hydrogel (c-DN gel) was fabricated. The c-DN gel can be connected to an external circulation system for a vascular-like perfusion through the inner channel. The c-DN gel can be connected to an external circulation system for a vascular-like perfusion through the inner channel. This system not only enabled a sustainable supply of monomers during mechanoradical polymerization s but also replenished the water loss and prevented drying of gels in the air.

We demonstrated that the system can support the repetitive self-strengthening of DN gels that lasted for hours in deoxygenated air. The metabolic-like growth of c-DN gels in response to cyclic loading exhibited similarities to the strengthening and hypertrophy of muscles supported by the vascular circulation. Analogous to muscle growth, which is sustained by nutrients from blood vessels, vascular perfusion in the c-DN gel cleared obstacles for replenishing monomers during the self-growing process.

Instead of requiring underwater conditions, the c-DN gel can obtain monomers from the circulatory flow of an independently controllable solution supply. Through the diffusion of monomers into the permeable c-DN gels, mechanochemical growth can be readily tuned by changing the monomer concentration flowing through the channel, allowing us to directly control the mechanical growth and trace the corresponding variations in the chemical components.

The tunable duration time of the monomer supply in the channel also helped to decipherer the interplay between mechanoradical initiated polymer growth and self-strengthening. We observed a pronounced difference between the increasing trend of the polymer content and the mechanical parameters. Using Raman spectroscopy, we detected discrepancies in the kinetics of polymer growth and mechanical strengthening, deciphered unique features of mechanochemical reaction in DN gels including the extremely long-living radicals and delayed mechanical strengthening through a desirable feedback loop. Besides, by quantifying both monomer diffusion and in-situ polymerization area, the lifetime of the network-trapped mechanoradical is observed to be about 10 minutes. Benefiting from these long-existing macroradicals and the self-sustainable channel structure, the mechanochemical reactions in c-DN hydrogel may promote their use in applications such as soft robotics, real-time spectrum monitoring, and mechano-chemical reactors.

List of Publications

Gumi Wei, Yumeko Kudo, Takahiro Matsuda, Zhi Jian Wang, Qi Feng Mu, Daniel R. King, Tasuku Nakajima, Jian Ping Gong, Sustainable Mechanochemical Growth of Double-Network Hydrogels Supported by Vascular-like Perfusion, *Mater. Horiz*., **2023**, 10, 4882-4891

Acknowledgement

All praises to Prof. GONG for letting me to complete this PhD journey with her blessings, guidance, merciful and incomparable support.

Special appreciation to Dr. KING with his full support on the very first day of my enrollment. His patience, determination and motivations are never to be forgotten and I am truly grateful for that.

I am very grateful to one of my supervisor: Dr. NAKAJIMA, for his precious time for discussions and progressive meetings as well as advising my presentation and experiments. A very excellent recommend of quantifying the self-growth amount by FTIR or Raman was advised from him, I really appreciate that.

I would like to thank members in the lab team: Ms. Y. KUDO for her help in the microstructural investigations; Dr. T. MATSUDA for his help in providing suggestions about mechanoradical polymerizations and a thoroughly review of the manuscript before submission; Dr. Z. J. WANG for his time and efforts in assisting me in learning tension and compression tests carrying out in the glovebox, and detection of mechanoradical concentrations using UV-Visible absorption spectroscopy; Dr. Miléna and W.Q. YANG helped in POM experiments; Dr. X.Y. LI and Dr. D. SHI helped in SAXS analyses; Dr. FAN helped in rheology measurements; Dr. KIYAMA helped in contact angle measurements; many thanks also to the staffs including HANE-san, Dr. Y. KATSUYAMA, MATSUMOTO-san, people in the lab are all warm hearted and kindly help tricky problems in the lab.

Many thanks also to Nikon Imaging Center, Research Institute for Electronic Science, Hokkaido university (NIC@HU), for the dedicate assistance from the technical stuff, Kentarou KOBAYASHI in measuring the fluorescent results.

I will also remember all the friends I met in Hokkaido University, for the good memories they build together with me, I saw their courage and motivational spirits to life, for example Dr. LIU, who dares to drive hundreds of miles away from Sapporo to east of Hokkaido when she just get her driving license. I can still remembered the feeling when I heard this news, on her car. I saw her manipulating buttons with mistakes and mess, my heart never beats that fast.

I would like to thank Ministry of Education, Culture, Sports, Science and Technology (MEXT) for the scholarship support.

Last but not least, I am grateful to my beloved family and parents for their continuous support and love.

Gumi WEI

Graduate School of Life Science

Hokkaido University, Japan

March 2024